September 11, 1996

MEMORANDUM TO: Jack R. Strosnider, Chief
Materials and Chemical Engineering Branch
Division of Engineering, NRR

FROM: Michael E. Mayfield, Chief *AC Millman /for*
Electrical, Materials and Mechanical Engineering Branch
Division of Engineering Technology, RES

SUBJECT: STEAM GENERATOR TUBE FLAW DISTRIBUTIONS

As promised in J. Muscara's e-mail message to you of September 5, 1996, attached is a summary report on "Flaw Distribution for Example Plants." The report was prepared by Dominion Engineering Inc. (DEI) under a subcontract to the ANL steam generator tube integrity research program. The report is based on the extensive knowledge and data bases at DEI on steam generator tube degradation, inservice inspection (ISI) results from many plants over many operating cycles, and on DEI's extensive work on statistical analyses of steam generator tube degradation.

The initial draft report and calculations from DEI conducted under this effort were reviewed by a panel of experts comprised of W. Shack (ANL), R. Kurtz (PNNL), J. Begley (APTECH), C. Laire (LABORELEC,Belgium), and L. Cizelj (Jozef Stefan Institute, Slovenia). A meeting was held on August 26, 1996, where the DEI principal investigator presented results of the study to the panel members, and the members provided comment and input based on their review of the initial report and the presentation. Two key recommendations from the panel were that: a) the detected flaw distributions obtained from the ISI results should be adjusted to include the effect of inspection reliability, probability of flaw detection, and sizing accuracy, to arrive at estimated "actual" flaw distributions; and b) the flaws produced by loose parts should be included.

The attached summary report provides examples of flaw distributions associated with the important degradation mechanisms that would be experienced by a typical plant with Model 51 steam generators containing low temperature mill annealed alloy 600 tubes with Wextex expansions. The recommendations of the panel members are included in the calculations for the flaw distributions in the summary report. These flaw distributions can be used by the NRR staff who are conducting evaluations of tube failure and rupture probabilities and of risk in conjunction with rulemaking activities underway for steam generators.

The full report will contain detailed discussions of the methodology and assumptions used for estimating flaw distributions, the historical ISI and degradation data from different plants that is used to develop the distributions, and additional example flaw distributions for other typical steam generator designs and flaw degradation mechanisms. We expect this full report to be completed by October 1, 1996.

Attachment: As stated

Distribution: w/o Attachment

Signature File (LCS)	Branch Reading File	T.Speis	D.Morrison
B.Sheron (NRR)	A.Thadani (NRR)	R.C.Jones (NRR)	
J.E.Donoghue (NRR)	S.Long (NRR)	T.Reed (NRR)	E.Murphy (NRR)

DOCUMENT NAME: G:\MEB\MUSCARA\FLWDIST2.NRR
To receive a copy of this document, indicate in the box: "C" = Copy without attachment/enclosure "E" = Copy with attachment/enclosure "N" = No copy

OFFICE	EMMEB	E	C\EMMEB		D\DET					
NAME	J Muscara		G.Millman		M.Mayfield					
DATE	09/ 11 /96		09/ 11 /96		09/ 11 /96					

9609200114 960911 PDR ADOCK 05000 P PDR

OFFICIAL RECORD COPY RES File Code: IB-9

Flaw Distributions for Example Plants

1. Objective

The objective of this document is to provide distributions of flaws in steam generator tubes of example plants for use in evaluations of the likelihood of leakage or burst under severe accident and design basis accident conditions.

2. Background

In response to ANL PO No. 063168, DEI is preparing a report that describes methods for estimating the distributions of flaws by size of various types in PWR steam generator tubes. Appendices A and B of the report will provide much of the historical data regarding flaws that are needed to determine the flaw distributions for different plants. Appendix C of the report will contain numerical examples for a moderately affected, severely affected, and lightly affected plant.

This preliminary report provides examples of flaw distributions associated with a number of important degradation mechanisms. It contains a summary of results from the full report.

3. Contents and Organization of Information

The flaw distribution information attached to this summary document is organized in six parts, which are largely taken from Appendix C of the main report for the project. Each part treats a separate degradation mechanism. The mechanisms covered are the following:

1. Circumferential SCC at the TTS (Mostly PWSCC)
2. Circumferential ODSCC at Dents at TSPs
3. Freespan Cracks
4. Sludge Pile IGA/SCC
5. Axial ODSCC at TSPs (non dented)
6. Flaws due to Loose Parts

For each flaw type, appropriate figures are assembled from Appendices A, B, and C of the full report and supplemented by additional figures and evaluations so as to present a coherent whole for that flaw type. The typical organization is as follows:

- Intercept time and Weibull slope data, which are used to estimate numbers of cracks, are taken from Appendix A.
- Monte Carlo evaluations to determine the numbers of tubes with flaws for

the three cases are taken from Appendix C.

- Flaw distribution data based on representative NDE and pulled tube data are taken from Appendix B. These data are adjusted as appropriate to reflect measurement error and probability of detection (POD).

- For cases where defects have only one dimension, the adjusted flaw distributions are applied to the numbers of tubes with defects to distribute the flaws by size "bins." In cases where the flaws have two dimensions (length and depth), this is not practical. In these cases analytical expressions are given for the length and depth distributions.

4. Summary Table

Some of the key results for the six flaw types are shown on Table 1.

Table 1. Flaw Distributions for Hypothetical Example Cases

Plant Characteristics

No. of Steam Generators:	3
No. of Tubes = 3*3388 =	10164
Tube Material	LTMA 600
Expansion Method:	Wextex
Hot Leg Temperature, °F:	605
BOC EFPY:	14
EOC EFPY:	15.2

		Moderately Affected Plant	Severely Affected Plant	Lightly Affected Plant
1. Circumferential SCC at TTS (Mostly PWSCC)				
Number of tubes with Circ. SCC at TTS at 15.2 EFPY (Note 1) =		7.0	46.3	1.4
Gamma distribution parameters for crack arc length;				
arc length in degrees (Note 2):*	α =	2.84	2.84	2.84
	β =	28.1	28.1	28.1
2. Circumferential ODSCC at Dents at TSPs				
Number of tubes with cracks at15.2 EFPY Note 1) =		4.2	40.1	0.32
Gamma distribution parameters for crack arc length;				
arc length in degrees (Note 2):*	α =	34.4	34.4	34.4
	β =	3.23	3.23	3.23
3. Free Span ODSCC				
Number of tubes with cracks at 15.2 EFPY (Note 1) =		5.2	60.2	1.7
Gamma distribution parameters for length, in. (Note	α =	0.17	0.17	0.17
	β =	0.88	0.88	0.88
Gamma distribution parameters for depth, % wall (No	α =	17.0	17.0	17.0
	β =	3.80	3.80	3.80
4. IGA/SCC in Hot Leg Sludge Pile				
Number of tubes with cracks at 15.2 EFPY (Note 1) =		39.6	60.2	18.9
Gamma distribution parameters for length, in. (Note	α =	0.17	0.17	0.17
	β =	0.88	0.88	0.88
Gamma distribution parameters for depth, % wall (No	α =	17.0	17.0	17.0
	β =	3.80	3.80	3.80
5. Axial ODSCC at TSPs				
Number of tubes with ODSCC (0.85 volt level) at 15.2 EFPY (note 1		569.7	6024.6	131.1
Gamma distribution parameters for depth of 0.75" long cracks;				
depth in % of wall:	α =	0.770	0.770	0.770
	β =	4.480	4.480	4.480
6. Flaws Due to Loose Parts				
Number of tubes with flaws at 15.2 EFPY =		0.7	0.7	0.7
Gamma distribution parameters for length, in.:*	α =	1.900	1.900	1.900
	β =	0.458	0.458	0.458
Gamma distribution parameters for depth, % wall:*	α =	2.275	2.275	2.275
	β =	17.235	17.235	17.235

*For macrocracks. Macrocracks consist of series of 0.3" thru-wall cracks separated by 0.05" long ligaments.

*For individual macrocracks. There are typically two near thru-wall diametrically opposed macrocracks per cracked location. See Figures C-6 and 7 for distribution of combined crack lengths.

* Crack length and depth distributions are assumed to be independent.

* Crack length and depth distributions are assumed to be independent.

* Crack length and depth distributions are assumed to be independent.

* Flaw length and depth distributions are assumed to be independent.

Notes

1. Numbers of tubes are totals that reflect adjustment for detection efficiencies.
2. Gamma distributions are for "actual" flaws, i.e., after adjustment for measurement error and POD.

September 6, 1996

1. Circumferential SCC at TTS (Mostly PWSCC)

The distribution of times to detection of circumferential SCC at the TTS for Wextex units for a hot leg temperature of 605°F is shown on Figure A-3 (median time of 7.53 EFPY, 16th percentile time of 4.56 EFPY and 84th percentile time of 10.72 EFPY). The Weibull slopes for these plants are listed on Figure A-4A, and a Weibull fit to the slopes is shown on Figure A-4B (fitted median of about 3). The distributions for intercept times and slopes were used in a Monte Carlo evaluation of the type described in Section 5 to determine a distribution of the numbers of newly detectable flaws developing during the operating cycle, i.e., between 14.0 and 15.2 EFPY. A typical run for the Monte Carlo evaluation is shown on Figure C-1. Results of five runs, representing 5000 trials, are shown on Figure C-2. Figure C-2 shows median, 16th percentile and 84th percentile results for both fractions and numbers of tubes. These are taken as representing moderately affected, lightly affected and severely affected units respectively. The results for the three cases are as follows:

Case	Delta F %	Number of Tubes with Detectable Flaws at 15.2 EFPY
Moderate	0.045	5
Severe	0.32	33
Light	0.012	1

A typical distribution of measured crack arc lengths for TTS circumferential cracks in tubes with Wextex expansions is shown in Figures B-3A and B-3B. The gamma distribution parameters for that distribution are: $\alpha = 6.06$, $\beta = 17.33$. These cracks are characterized as being essentially through wall, but as being made up of segments about 0.3 inches in length separated by uncracked ligaments of 0.050 inches in length.[1]

Based on a report with pulled tube to RPC measurement comparisons for two cracks,[2] RPC measurements for Wextex cracks appear to have a mean error of 6.0° (RPC overcalls the length), with a standard deviation of 5.7°. Based on data in the same report, together with engineering judgment, the POD for these defects was approximated as being zero at 25°, 0.95 at 75° and higher angles, with a straight line variation between these two values. The flaw size distribution was adjusted to reflect the measurement error and POD using the method described by Heasler.[3] The resulting estimated "actual" flaw size distribution is shown in Figures B-3C and B-3D. A "detection efficiency" was determined by setting it equal to the integral of the probability of detection times the actual distribution

divided by the integral of the actual size distribution. The integrals were taken for all flaws greater than 20°.

The numbers of flaws expected at the end of the operating cycle, i.e., at 15.2 EFPY, were then distributed in size using the actual flaw size distribution of Figures B-3C and B-3D. The results of this distribution are shown in Figure C-3. Note that the total number of flaws was increased from the predicted number of detectable flaws using the efficiency factor determined above. As shown on Figure C-3, the predictions indicate that there are no large cracks, e.g., of 250° arc length or more, even for the severe case. In addition, as noted earlier, destructive examinations indicate that there will be ligaments present about every 0.3 inches (about 40°) in the large cracks.

---

1 North Anna Unit 1 Steam Generator Operating Cycle Evaluation, Westinghouse WCAP-13035, August 1991, forwarded by Virginia Electric and Power Company letter dated August 30, 1991, in NRC PDR, 9109100132 910880, Docket No. 50-338.

2 Ibid.

3 P. G. Heasler, et al., Analysis Before Test: Estimation of Fabrication Defect Rates in Reactor Pressure Vessels, Draft PNL report for NRC, Nov. 1994.

Figure A-3. Industry Time to Detection of Circumferential TTS SCC (ID/OD) - Median Rank Analysis - Wextex Plants with 600 LTMA Tubing

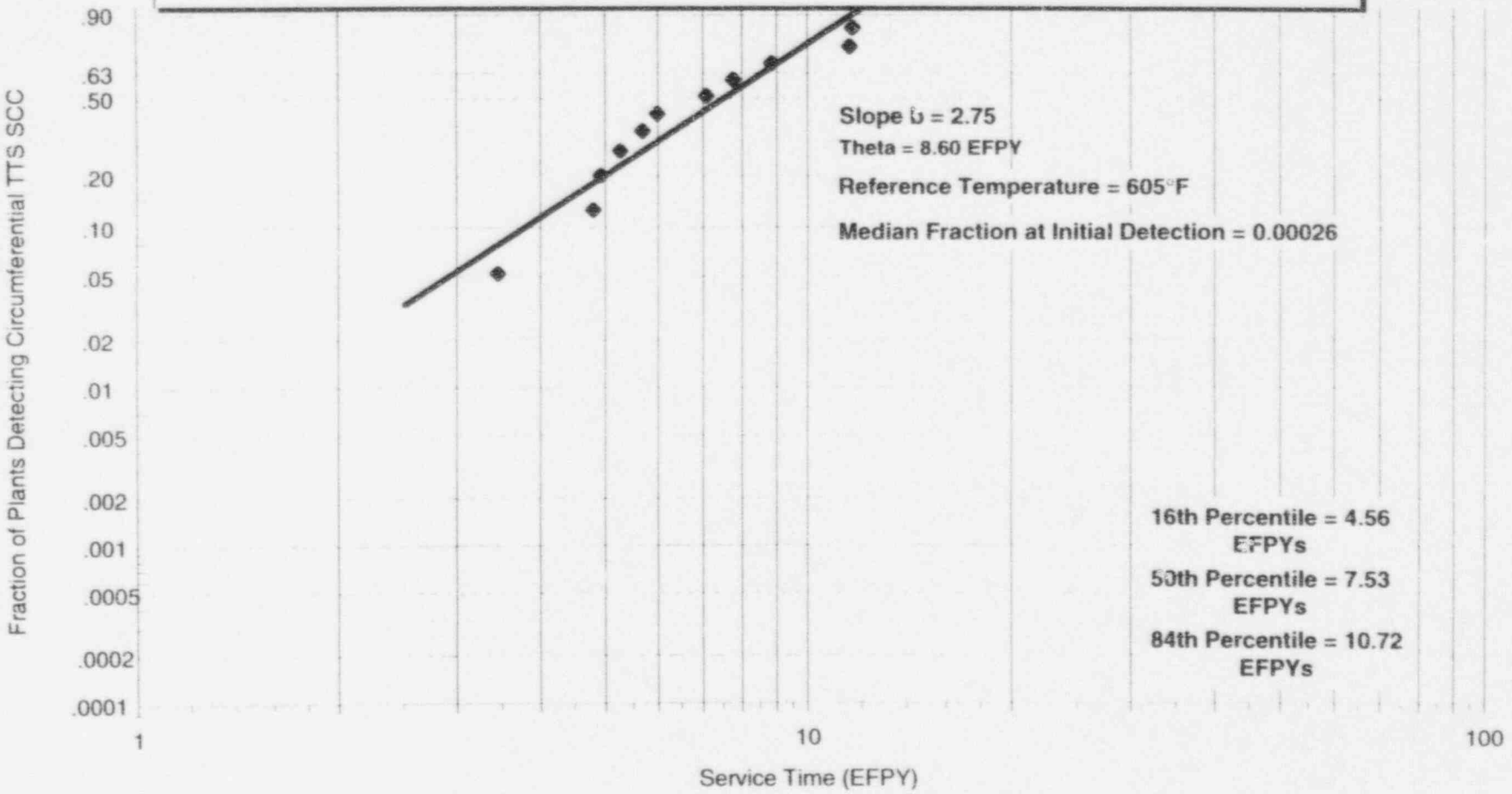

Figure A-4A. Weibull Slopes for Wextex Plants with Circumferential TTS SCC (before peening)

			Median Slope =	**2.82**	
			16% Slope =	**2.13**	
			84% Slope =	**4.16**	
No.	**Plant**	**Slope**	**% Error**	**Points**	**Median Rank**
1	A	2.00	9.4	4	0.130
2	B	2.78	32.6	6	0.315
3	C	2.82	6.6	3	0.500
4	D	3.35	8.2	3	0.685
5	E	4.32	21.2	5	0.870

5 < Number of Plants

Updated: Jul-96

Dominion Engineering, Inc.

Figure A-4B. Weibull Fit to Wextex Slopes

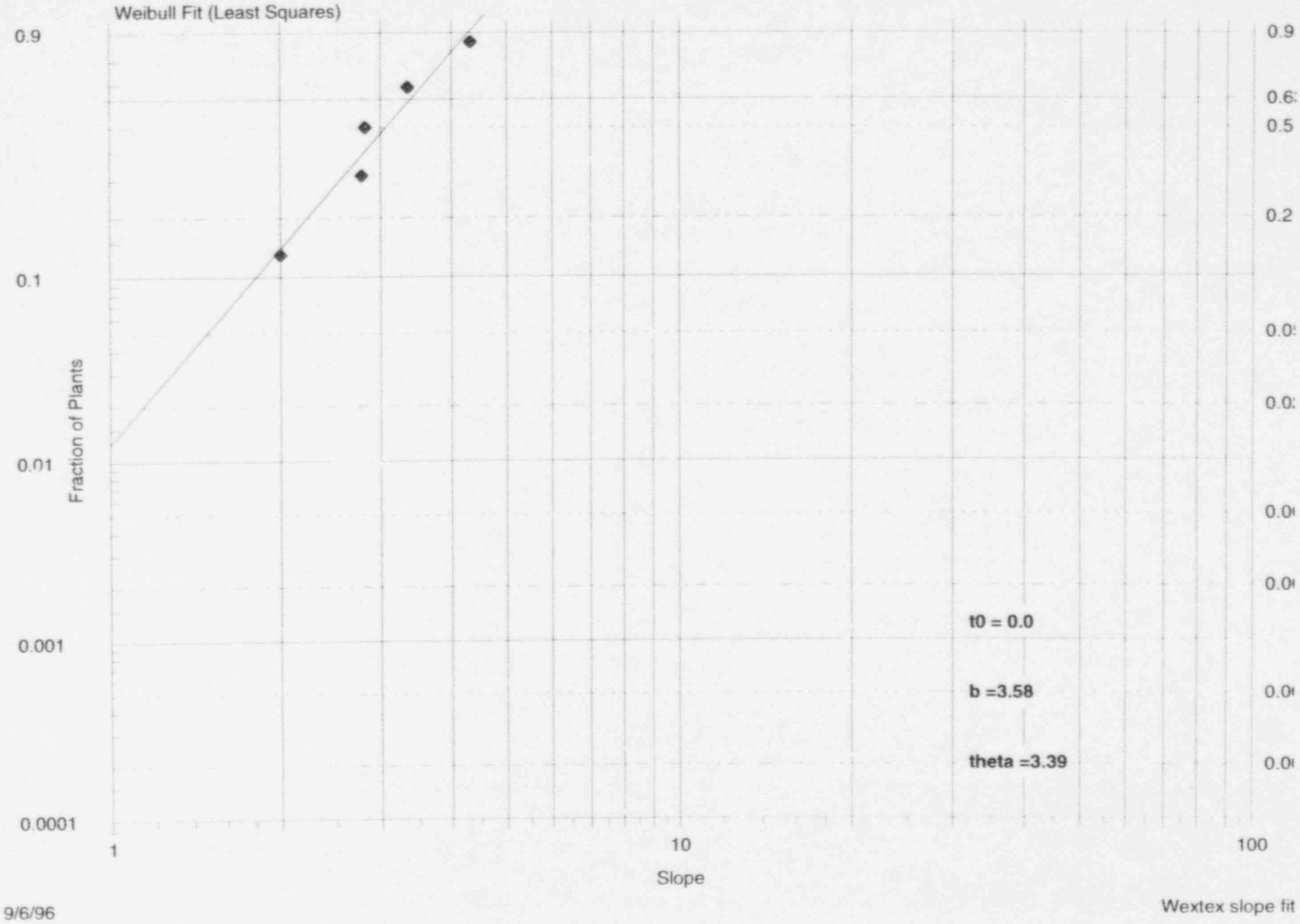

9/6/96

Wextex slope fit

Figure C-1. Weibull Distribution Monte Carlo - Wextex TTS Circumferential Flaws

Distributions

Slope	b		Time to 0.026% Failures	t0%	Susceptible Fraction	ß	
Type [1]	Weibull		Type [1]	Weibull	Type [1]		
Slope	3.58		Slope	2.75	ß	1	
Theta	3.39		Theta	8.604		10	
			error				
			error				
Min b	1		Min t0%	0.00	Min ß	0.001	
Max b	8		Max t0%	1751.6	Max ß	1	
Normalization	1.01		Normalization	1.00	Normalization		
Start Trunc	0.0126		Start Trunc	0.0000	Start Trunc		

Times of Interest

14.0	EFPY
15.2	EFPY

Results
(1000 trials)

Median Delta F	16%ile Delta F	84%ile Delta F
0.000446	0.000114	0.00296

Figure C-2. Wextex Delta F Runs

	Median Delta F	16%ile Delta F	84%ile Delta F
	0.000483	0.000119	0.00399
	0.000473	0.000112	0.00346
	0.000446	0.000121	0.00292
	0.000408	0.000115	0.00314
	0.000420	0.000114	0.00259
mean	0.000446	0.000116	0.00322
delta N	4.5	1.2	32.7

Figure B-3A. North Anna 1 1991 TTS Circumferential Crack Arc Lengths

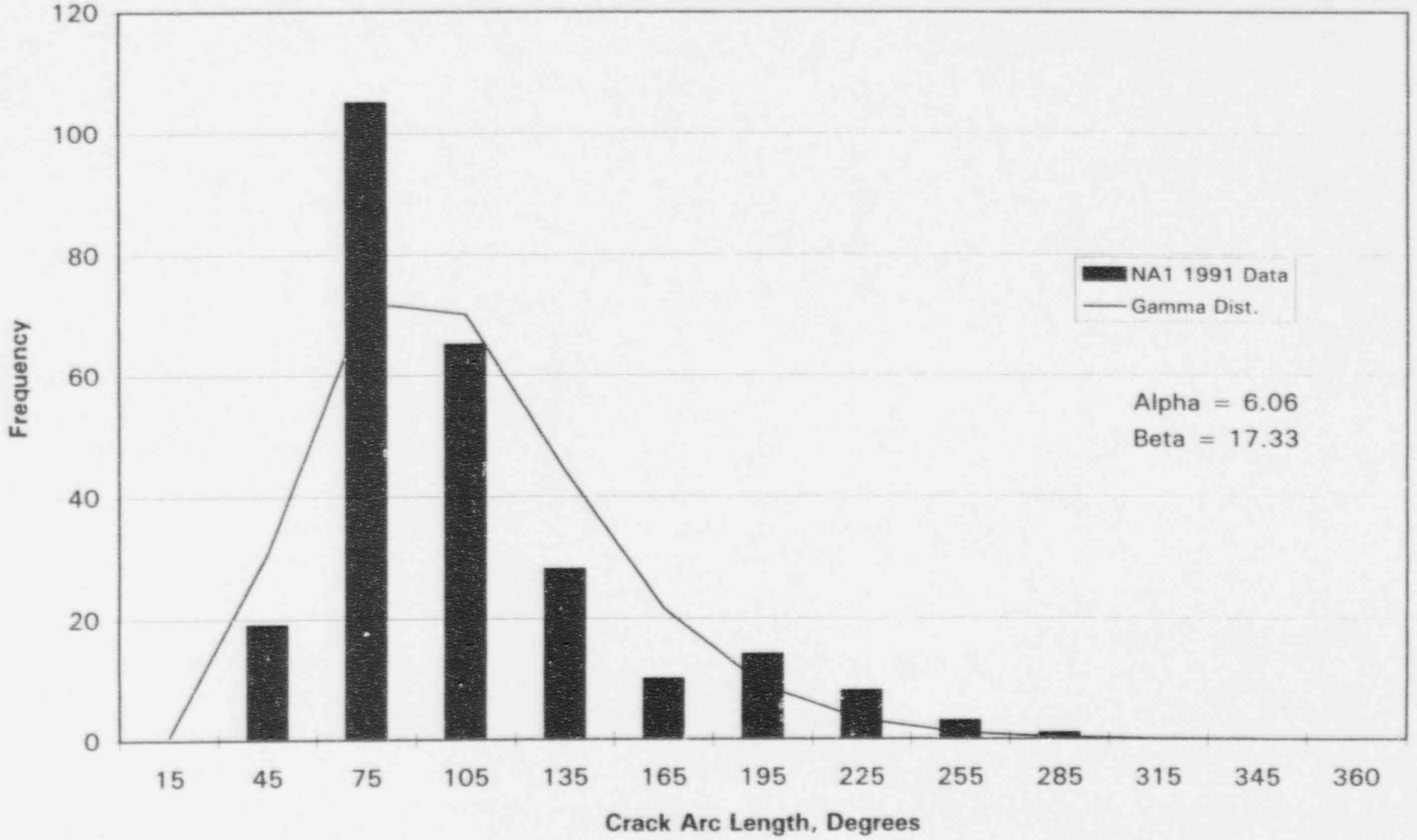

Figure B-3B. North Anna 1 1991 TTS Circumferential Crack Arc Lengths

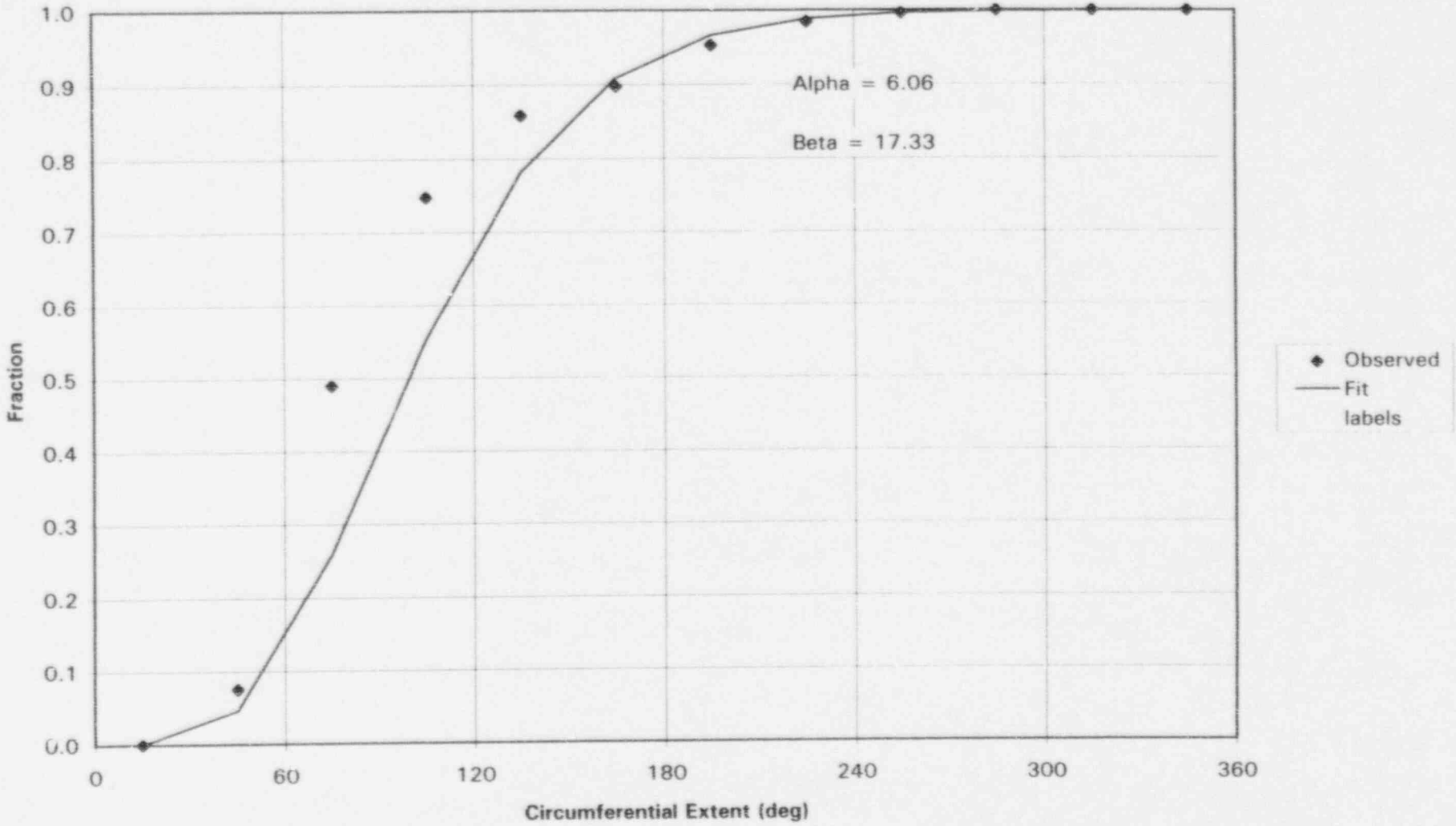

Figure B-3C. TTS Circumferential Crack Arc Lengths

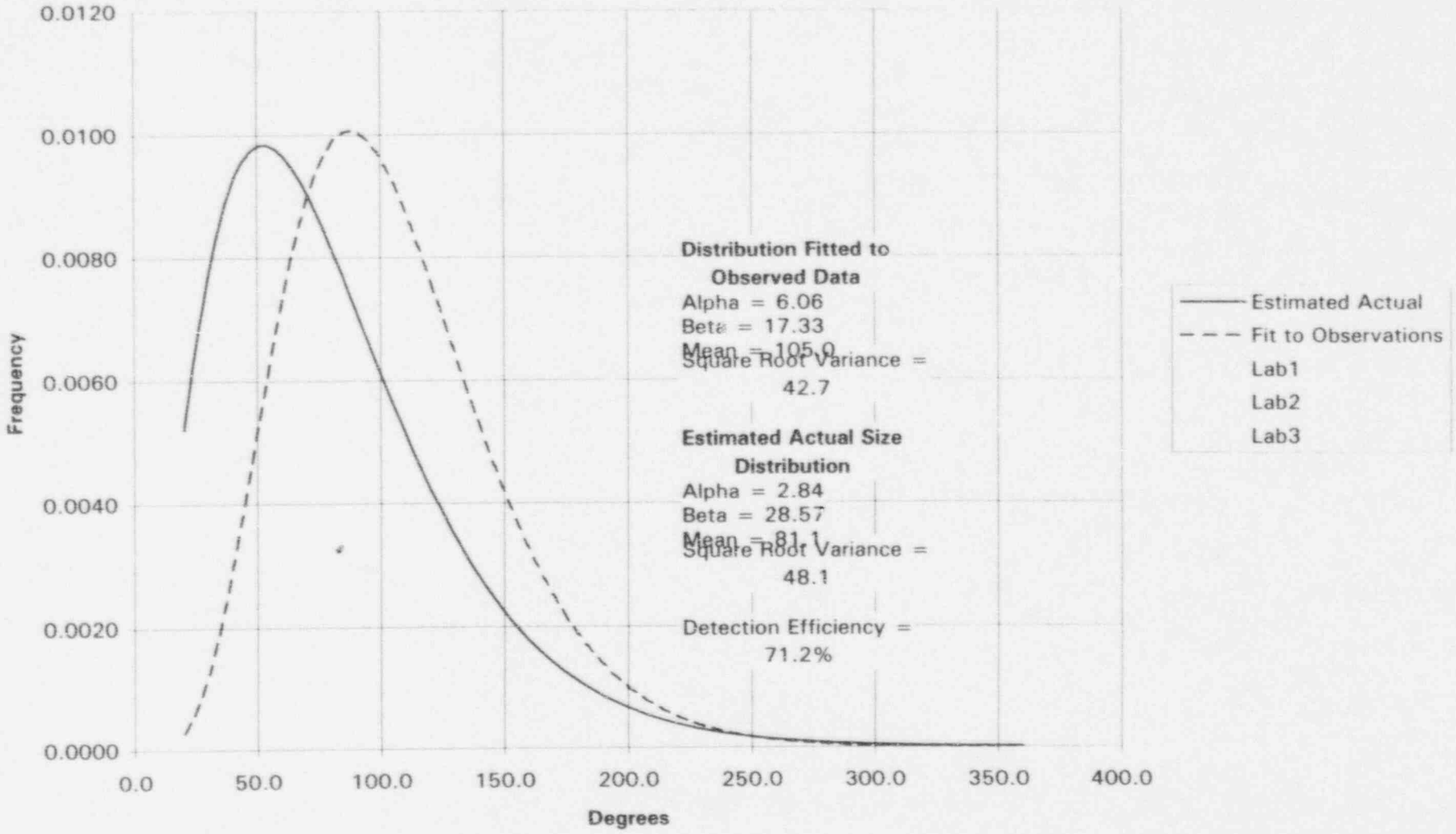

Figure B-3D. TTS Circumferential Crack Arc Lengths

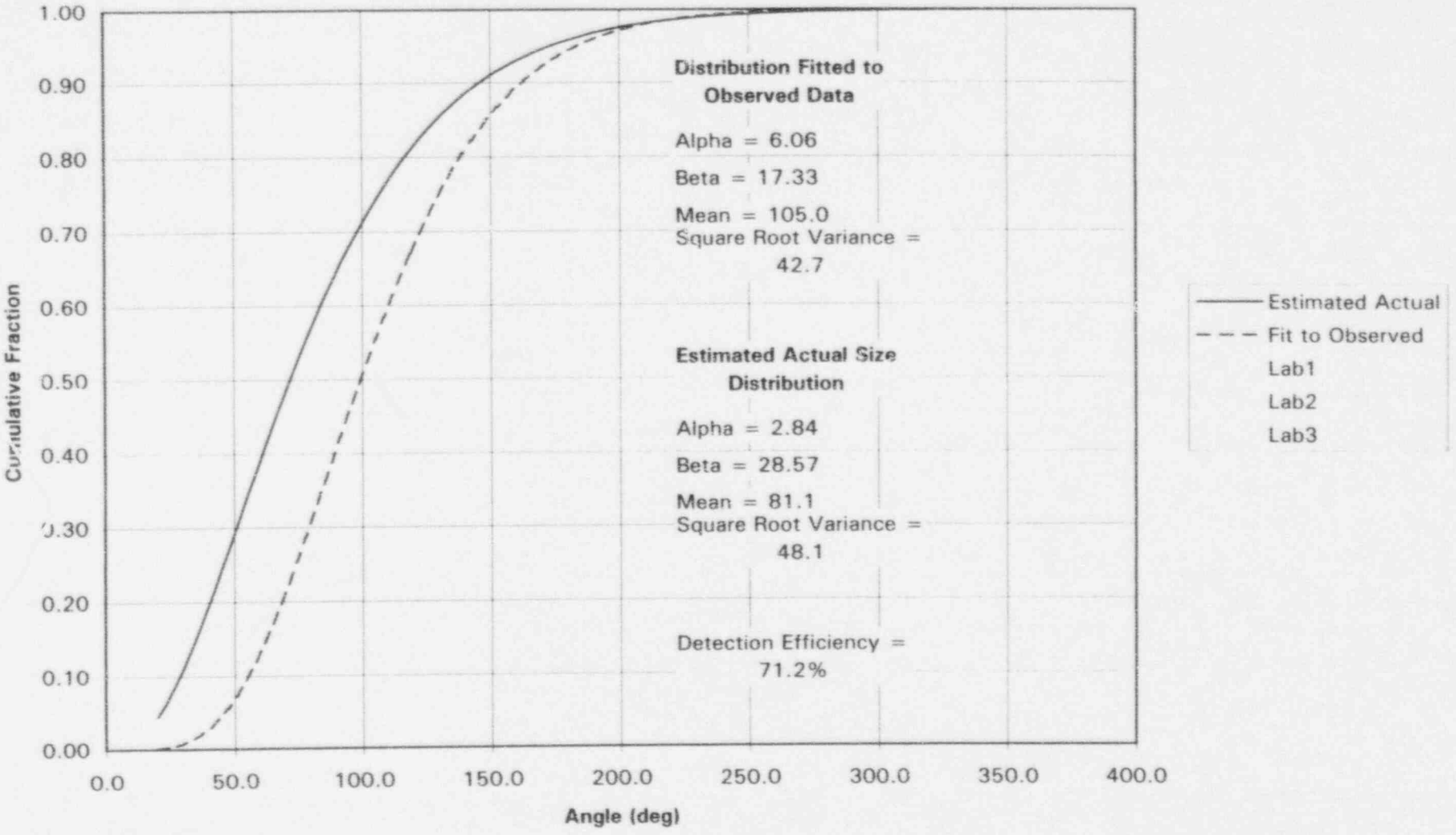

Figure C-3, Binned Flaw Distributions - Circumferential Crack Arc Lengths at TTS

Case:		Moderate	Severe	Light
Detected Flaws:		5.0	33	1
Detection Efficiency:	0.712			
Total Flaws:		7.0	46.3	1.4
Alpha	2.84			
Beta	28.57			
Arc Length Degrees	F	No. in Bin	No. in Bin	No. in Bin
25	0.074	0.2	1.4	0.04
30	0.110	0.3	1.7	0.05
35	0.151	0.3	1.9	0.06
40	0.195	0.3	2.1	0.06
45	0.243	0.3	2.2	0.07
50	0.292	0.3	2.3	0.07
55	0.341	0.3	2.3	0.07
60	0.389	0.3	2.3	0.07
65	0.437	0.3	2.2	0.07
70	0.483	0.3	2.1	0.06
75	0.528	0.3	2.1	0.06
80	0.570	0.3	1.9	0.06
85	0.609	0.3	1.8	0.06
90	0.646	0.3	1.7	0.05
95	0.681	0.2	1.6	0.05
100	0.712	0.2	1.5	0.04
105	0.742	0.2	1.4	0.04
110	0.769	0.2	1.2	0.04
115	0.793	0.2	1.1	0.03
120	0.815	0.2	1.0	0.03
125	0.836	0.1	0.9	0.03
130	0.854	0.1	0.8	0.03
135	0.870	0.1	0.8	0.02
140	0.885	0.1	0.7	0.02
145	0.898	0.1	0.6	0.02
150	0.910	0.1	0.5	0.02
155	0.921	0.1	0.5	0.01
160	0.930	0.1	0.4	0.01
165	0.939	0.1	0.4	0.01
170	0.946	0.1	0.3	0.01
175	0.953	0.0	0.3	0.01
180	0.958	0.0	0.3	0.01
185	0.964	0.0	0.2	0.01
190	0.968	0.0	0.2	0.01
195	0.972	0.0	0.2	0.01
200	0.976	0.0	0.2	0.00
205	0.979	0.0	0.1	0.00
210	0.981	0.0	0.1	0.00
215	0.984	0.0	0.1	0.00
220	0.986	0.0	0.1	0.00

Figure C-3. Binned Flaw Distributions - Circumferential Crack Arc Lengths at TTS

Case:		Moderate	Severe	Light
Detected Flaws:		5.0	33	1
Detection Efficiency:	0.712			
Total Flaws:		7.0	46.3	1.4
Alpha	2.84			
Beta	28.57			
Arc Length Degrees	F	No. in Bin	No. in Bin	No. in Bin
225	0.988	0.0	0.1	0.00
230	0.989	0.0	0.1	0.00
235	0.991	0.0	0.1	0.00
240	0.992	0.0	0.1	0.00
245	0.993	0.0	0.0	0.00
250	0.994	0.0	0.0	0.00
255	0.995	0.0	0.0	0.00
260	0.995	0.0	0.0	0.00
265	0.996	0.0	0.0	0.00
270	0.997	0.0	0.0	0.00
275	0.997	0.0	0.0	0.00
280	0.997	0.0	0.0	0.00
285	0.998	0.0	0.0	0.00
290	0.998	0.0	0.0	0.00
295	0.998	0.0	0.0	0.00
300	0.999	0.0	0.0	0.00
305	0.999	0.0	0.0	0.00
310	0.999	0.0	0.0	0.00
315	0.999	0.0	0.0	0.00
320	0.999	0.0	0.0	0.00
325	0.999	0.0	0.0	0.00
330	0.999	0.0	0.0	0.00
335	0.999	0.0	0.0	0.00
340	1.000	0.0	0.0	0.00
345	1.000	0.0	0.0	0.00
350	1.000	0.0	0.0	0.00
355	1.000	0.0	0.0	0.00
360	1.000	0.0	0.0	0.00
	sum =	6.7	44.3	1.3

2. Circumferential ODSCC at Dents at TSPs

The amount of denting at TSPs of Model 51 steam generators with Wextex expansions varies from just a few tubes to 100% of the tubes being affected, and several plants have about 25% of their tubes affected. A denting rate of 10% is considered to be a moderate rate for this group of units, with 100% dented at severely affected units and about 1% at lightly affected units.

As discussed in Appendices A and B, the experience of North Anna 1 is used as a basis for this prediction, since the experience at North Anna 1 was the best characterized. The results for North Anna 1 are adjusted to reflect the lower temperature of the example plant (605°F versus 615°F). As indicated in Appendix A, the North Anna experience indicates that this type of degradation is expected to reach a level of 1% of the tubes with dents at about 7.6 EFPY at a hot leg temperature of 616°F Adjusting this to 605°F using an activation energy of 54 Kcal/mole results in this mode reaching 1% of dented tubes at the example plant at 12.2 EFPY. This is taken as the median intercept time. A distribution for the intercept time for this mode is not available. However, experience with other modes indicates that it is reasonable to assume that a standard deviation change occurs at about a factor of 1.5 in time, such that 16% of the plants are expected to experience this mode at 12.2/1.5 = 8.1 EFPY and 84% of the plants by 1.5 x 12.2 = 18.3 EFPY.

As discussed in Appendix A, a Weibull slope of 4 is considered to be a median slope for this mode. A distribution for slopes for this mode is not available. Based on variations in slopes for other modes, a standard deviation of about 2 is considered reasonable. This results in the 16% slope being 2 and the 84% slope being 6.

In summary, the parameters controlling this mode are as follows:

Percentile	Susceptible Fraction (% Tubes with Dents)	EFPY to 1% of Dented Tubes	Slope
16%	1	8.1	2
50%	10	12.2	4
84%	100	18.3	6

The above variables were modeled using log normal distributions for intercept times and susceptible fractions and a normal distribution for slopes, and then these distributions were used in a Monte Carlo evaluation of the type described in Section 5 to determine a distribution of the numbers of newly detectable flaws developing during the operating cycle, i.e., between 14.0 and 15.2 EFPY. A typical run for the Monte Carlo evaluation is shown on Figure C-4. Results of five runs representing 5000 trials, are shown on Figure

C-5. Figure C-5 shows median, 16th percentile and 84th percentile results for both fractions and numbers of tubes. These are taken as representing moderately affected, lightly affected and severely affected units respectively. The results for the three cases are as follows:

Case	Delta F, % (of whole tube bundle)	Number of Tubes with Detectable Flaws at 15.2 EFPY
Moderate (50%)	0.035	4
Severe (84%)	0.386	39
Light (16%)	0.003	0.3

The distribution of measured crack arc lengths for this mode of cracking found at North Anna 1 is shown on Figures B-14A and B-14B. The gamma distribution parameters for that distribution are: $\alpha = 16.71$, $\beta = 6.02$. These cracks are characterized as being essentially through wall, with most ligaments having been corroded away.[1]

Based on a report with pulled tube to RPC measurement comparisons for three cracks,[2] RPC measurements for ODSCC cracks at dented TSPs appear to have a mean error of -10.9° (RPC undercalls the length), with a standard deviation of 39°. Based on data in the same report, together with engineering judgment, the POD for these defects was approximated as being zero at 25°, 0.95 at 75° and higher angles, with a straight line variation between these two values. The flaw size distribution was adjusted to reflect the measurement error and POD using the method described by Heasler.[3] To accomplish this adjustment, the standard deviation for measurement error had to be reduced to 20° because the estimated 39° value led to an unrealistic actual crack size distribution. The resulting estimated "actual" flaw size distribution is shown in Figures B-14C and B-14D. A "detection efficiency" was determined by setting it equal to the integral of the probability of detection times the actual distribution divided by the integral of the actual size distribution. The integrals were taken for all flaws greater than 20°.

Based on pulled tube results from North Anna 1, it was assumed that two diametrically opposed cracks are present at the same elevation of each tube with a detected crack. It was further assumed that the sizes of the two cracks are independent, and that each independent crack size is controlled by the distribution shown on Figures B-14C and B-14D. To develop a distribution for the combined cracks, the sizes of each of the two cracks were determined using independent Monte Carlo sampling for each crack; these two sizes were then added to determine a total crack length for the trial. This was done for

1000 trials. The results of the distribution of total crack lengths for the two independent cracks combined are shown in Figure C-6.

The numbers of flaws of various total arc lengths expected at the end of the operating cycle, i.e., at 15.2 EFPY, were then determined. This was done starting with the numbers of tubes with detected flaws determined earlier. The numbers of detected flaws were divided by the detection efficiency to determine the total number of flaws. These flaws were then distributed into size bins using the distribution shown on Figure C-6. As shown on Figure C-7, the predictions indicate that some large cracks, i.e., of 270° arc length or more, are predicted as being present for the severe case. Since destructive examinations indicate that there few uncorroded ligaments in this morphology, this type of crack may involve the potential of causing significant leaks under accident conditions.

---

1 North Anna Unit 1 Steam Generator Operating Cycle Evaluation, Westinghouse WCAP-13035, August 1991, forwarded by Virginia Electric and Power Company letter dated August 30, 1991, in NRC PDR, 9109100132 910880, Docket No. 50-338.

2 Ibid.

3 P. G. Heasler, et al., Analysis Before Test: Estimation of Fabrication Defect Rates in Reactor Pressure Vessels, Draft PNL report for NRC, Nov. 1994.

Figure C-4. Weibull Distribution Monte Carlo - Circumferential Cracks at TSP Dents

Distributions

Slope	b		Time to 1.000% Failures	t1%	Susceptible Fraction	ß
Type [1]	Normal		Type [1]	Log Normal	Type [1]	Log Normal
Mean b	4.00		t1% @ mean	12.2	ß @ mean	0.1
Std.Dev. b	2.00		exp(Std.Dev.)	1.5	exp(Std.Dev.)	10
			Mean ln(t1%)	2.50	Mean ln(ß)	-2.30
			S.Dev. ln(t1%	0.41	S.Dev. ln(ß)	2.30
Min b	1		Min t1%	3.61	Min ß	0.001
Max b	8		Max t1%	41.2	Max ß	1
Normalization	1.10		Normalization	1.00	Normalization	1.22
Start Trunc	0.0668		Start Trunc	0.0013	Start Trunc	0.0228

Times of Interest

14.0	EFPY
15.2	EFPY

Results
(1000 trials)

Median Delta F	16%ile Delta F	84%ile Delta F
0.000367	0.000031	0.00343

Figure C-5. TSP Circ Delta F Runs

	Median Delta F	16%ile Delta F	84%ile Delta F
	0.000419	0.000031	0.00436
	0.000320	0.000025	0.00384
	0.000362	0.000027	0.00354
	0.000361	0.000033	0.00405
	0.000311	0.000027	0.00350
mean	0.000354	0.000029	0.00386
delta N	3.6	0.3	39.2

Figure B-14A. North Anna 1 1991 Dented TSP Circumferential Crack Arc Lengths

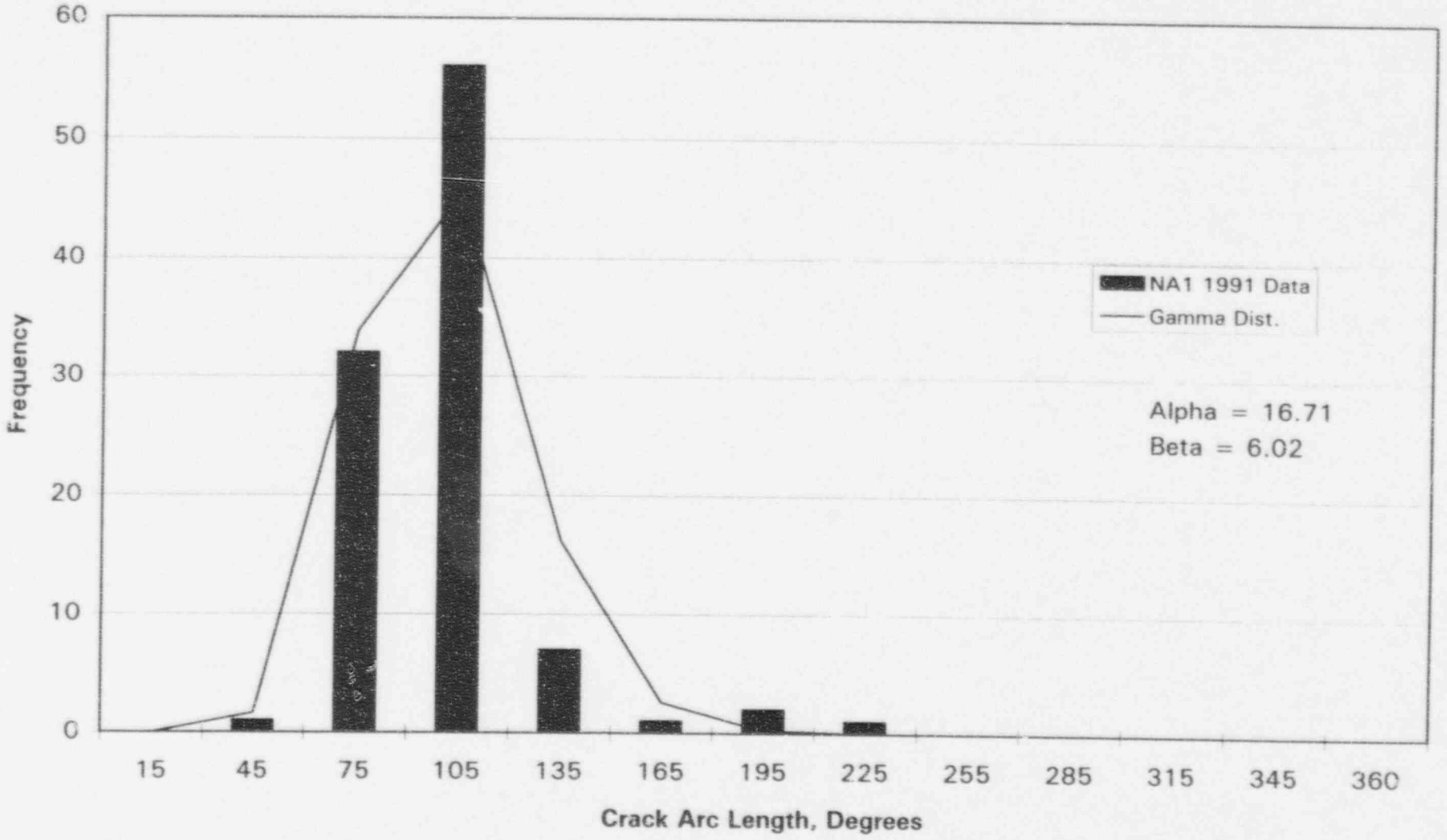

Figure B-14B. North Anna 1 1991 Dented TSP Circumferential Crack Arc Lengths

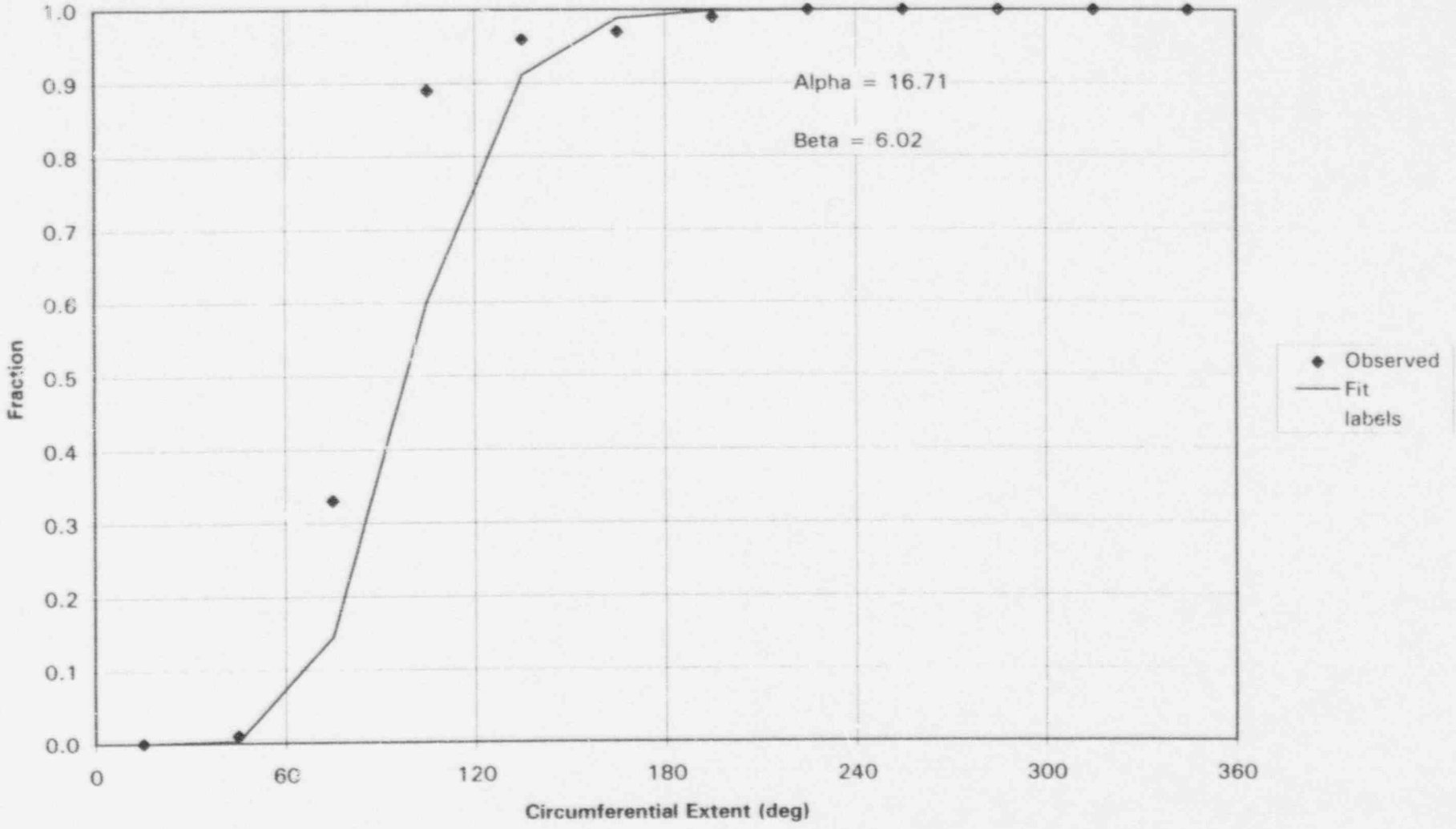

Figure B-14C. Dented TSP Circumferential Crack Arc Lengths

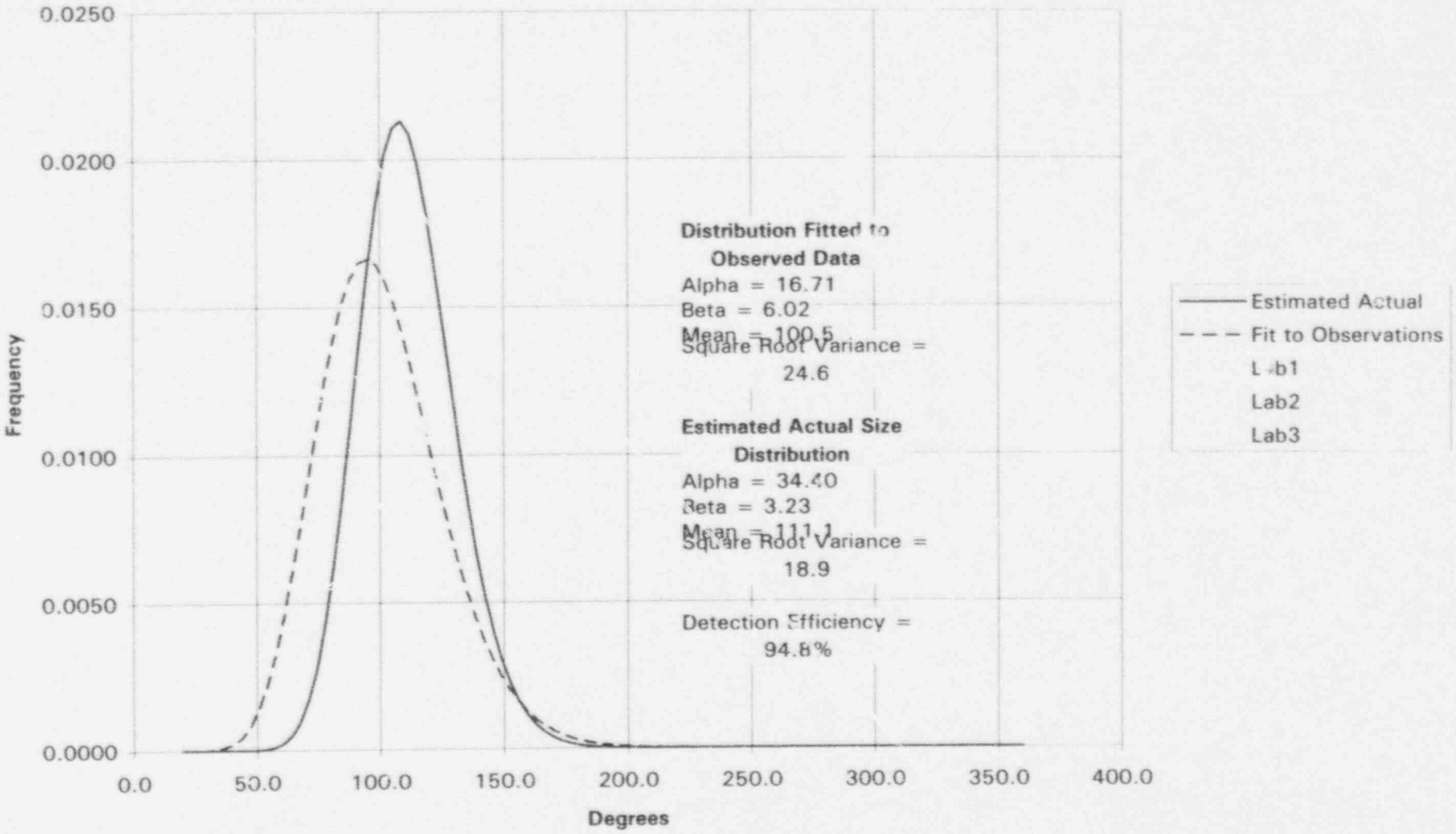

Figure E-14D. Dented TSP Circumferential Crack Arc Lengths

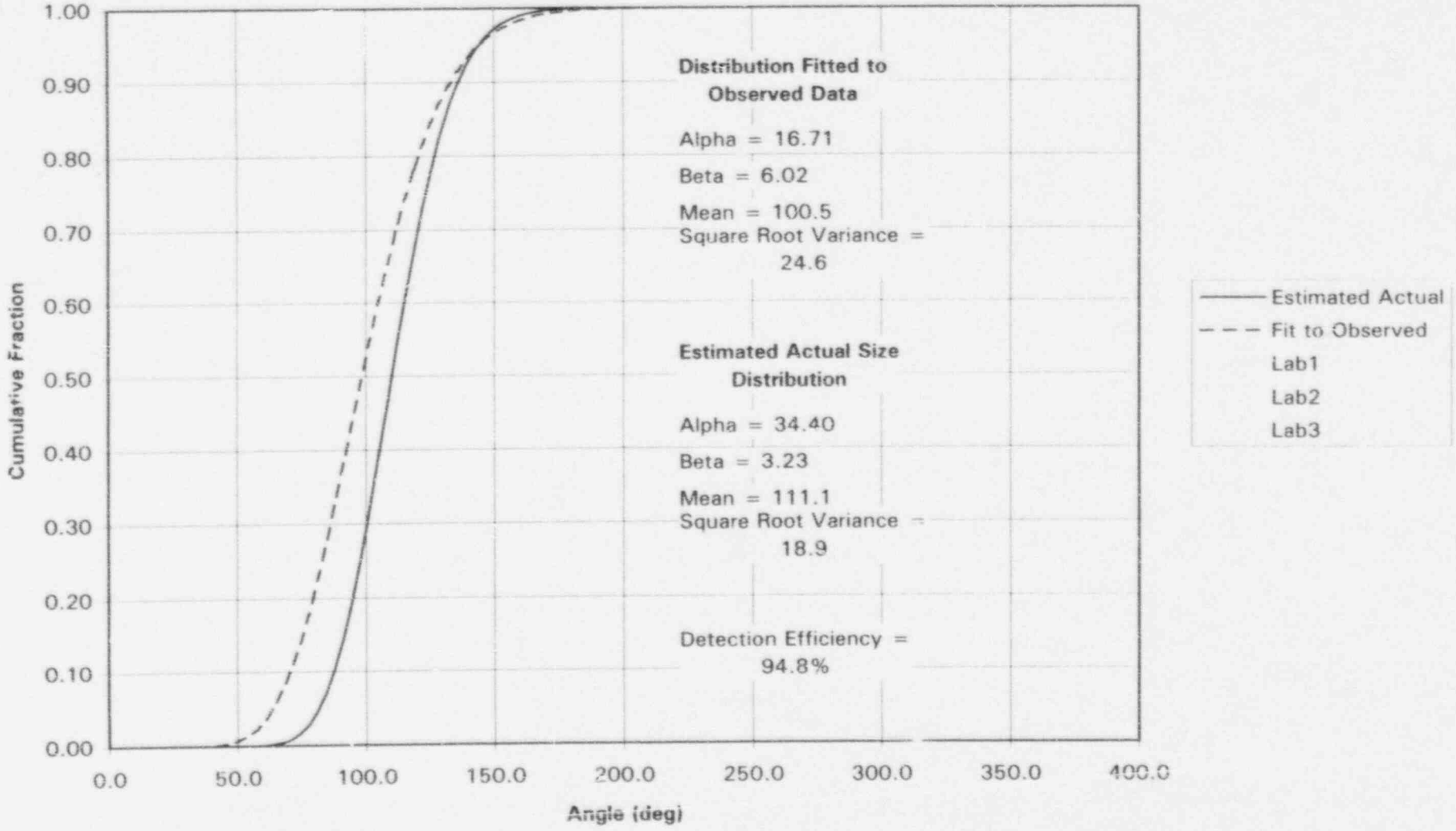

Figure C-6. Total Arc Length of Two Cracks at Dent

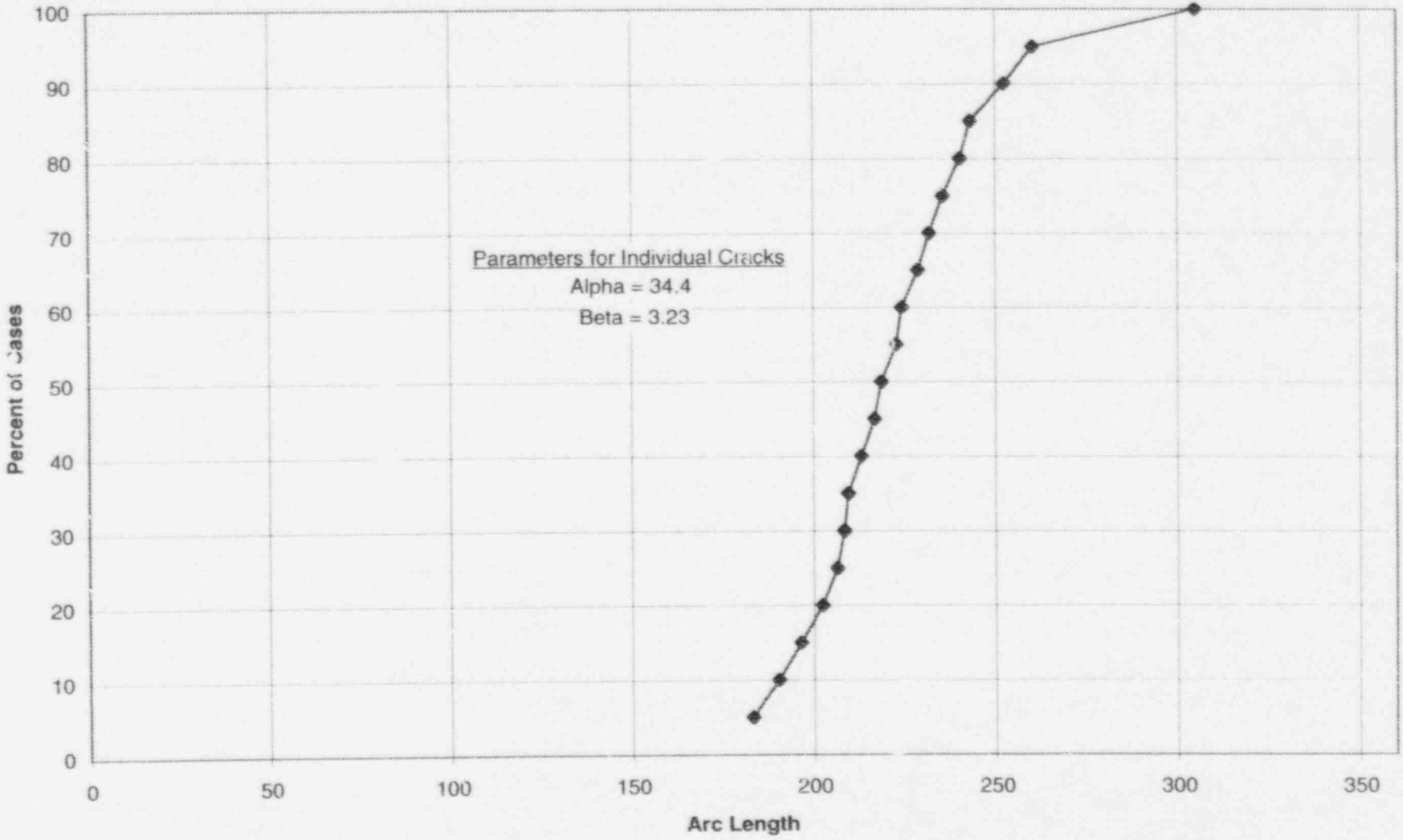

Figure C-7. Binned Flaw Distributions
Total Circumferential Crack Lengths at Dents
(Two Independent Cracks per TSP Location)

Case:		Moderate	Severe	Light
Detected Flaws:		4.0	38	0.3
Detection Efficiency:	0.948			
Total Flaws:		4.2	40.1	0.32

Arc Length Degrees	Count in 1100 trials	F	No. in Bin	No. in Bin	No. in Bin
25	0	0.000	0.0	0.0	0.00
30	0	0.000	0.0	0.0	0.00
35	0	0.000	0.0	0.0	0.00
40	0	0.000	0.0	0.0	0.00
45	0	0.000	0.0	0.0	0.00
50	0	0.000	0.0	0.0	0.00
55	0	0.000	0.0	0.0	0.00
60	0	0.000	0.0	0.0	0.00
65	0	0.000	0.0	0.0	0.00
70	0	0.000	0.0	0.0	0.00
75	0	0.000	0.0	0.0	0.00
80	0	0.000	0.0	0.0	0.00
85	0	0.000	0.0	0.0	0.00
90	0	0.000	0.0	0.0	0.00
95	1	0.000	0.0	0.0	0.00
100	2	0.000	0.0	0.0	0.00
105	3	0.000	0.0	0.0	0.00
110	3	0.000	0.0	0.0	0.00
115	4	0.000	0.0	0.0	0.00
120	9	0.000	0.0	0.0	0.00
125	17	0.000	0.0	0.0	0.00
130	28	0.000	0.0	0.0	0.00
135	42	0.000	0.0	0.0	0.00
140	64	0.000	0.0	0.0	0.00
145	86	0.000	0.0	0.0	0.00
150	109	0.000	0.0	0.0	0.00
155	142	0.000	0.0	0.0	0.00
160	173	0.000	0.0	0.0	0.00
165	213	0.000	0.0	0.0	0.00
170	266	0.000	0.0	0.0	0.00
175	324	0.000	0.0	0.0	0.00
180	374	0.000	0.0	0.0	0.00
185	452	0.053	0.2	2.1	0.02
190	499	0.099	0.2	1.8	0.01
195	568	0.148	0.2	2.0	0.02
200	626	0.200	0.2	2.1	0.02
205	677	0.283	0.3	3.3	0.03
210	736	0.369	0.4	3.5	0.03
215	796	0.440	0.3	2.9	0.02
220	842	0.519	0.3	3.2	0.02
225	873	0.579	0.3	2.4	0.02

Figure C-7. Binned Flaw Distributions
Total Circumferential Crack Lengths at Dents
(Two Independent Cracks per TSP Location)

Case:			Moderate	Severe	Light
Detected Flaws:			4.0	38	0.3
Detection Efficiency:		0.948			
Total Flaws:			4.2	40.1	0.32

Arc Length Degrees	Count in 1100 trials	F	No. in Bin	No. in Bin	No. in Bin
230	913	0.638	0.2	2.3	0.02
235	954	0.704	0.3	2.7	0.02
240	971	0.762	0.2	2.3	0.02
245	997	0.820	0.2	2.3	0.02
250	1014	0.874	0.2	2.2	0.02
255	1033	0.914	0.2	1.6	0.01
260	1047	0.938	0.1	1.0	0.01
265	1063	0.953	0.1	0.6	0.00
270	1069	0.959	0.0	0.2	0.00
275	1077	0.965	0.0	0.2	0.00
280	1082	0.971	0.0	0.2	0.00
285	1086	0.977	0.0	0.2	0.00
290	1087	0.983	0.0	0.2	0.00
295	1090	0.989	0.0	0.2	0.00
300	1092	0.995	0.0	0.2	0.00
305	1093	1.000	0.0	0.2	0.00
310	1094	1.000	0.0	0.0	0.00
315	1094	1.000	0.0	0.0	0.00
320	1096	1.000	0.0	0.0	0.00
325	1096	1.000	0.0	0.0	0.00
330	1097	1.000	0.0	0.0	0.00
335	1097	1.000	0.0	0.0	0.00
340	1097	1.000	0.0	0.0	0.00
345	1097	1.000	0.0	0.0	0.00
350	1097	1.000	0.0	0.0	0.00
355	1099	1.000	0.0	0.0	0.00
360	1100	1.000	0.0	0.0	0.00
		sum =	4.2	40.1	0.3

3. Freespan Cracks

The distribution of times to detection of free span SCC for Model 51 steam generators for a hot leg temperature of 605°F is shown on Figure A-17 (median time of 12.8 EFPY, 16th percentile time of 5.80 EFPY and 84th percentile time of 22.3 EFPY). The Weibull slopes for preheater plants are used since slopes are not available for feedring units; the preheater slopes are listed on Figure A-16A, and a Weibull fit to the slopes is shown on Figure A-16B (fitted median of about 3.1). The distributions for intercept times and slopes were used in a Monte Carlo evaluation of the type described in Section 5 to determine a distribution of the numbers of newly detectable flaws that develop during the operating cycle, i.e., between 14.0 and 15.2 EFPY. A typical run for the Monte Carlo evaluation is shown on Figure C-8. Results of five runs, representing 5000 trials, are shown on Figure C-9. Figure C-9 shows median, 16th percentile and 84th percentile results for both fractions and numbers of tubes. These are taken as representing moderately affected, lightly affected and severely affected units respectively. The results for the three cases are as follows:

Case	Delta F %	Number of Tubes with Detectable Flaws at 15.2 EFPY
Moderate	0.032	3
Severe	0.34	35
Light	0.007	1

As discussed in Appendix B, freespan cracking at Palo Verde 2 has been the best characterized, and is taken as being typical for the industry for cases where detailed inspections for freespan cracks are being performed. Consistent with the Palo Verde results, crack length and depth distributions are taken as being independent. A distribution of measured crack lengths for freespan cracks in Palo Verde 2 is shown in Figures B-10A and B-10B. The gamma distribution parameters for the freespan crack length distribution are: $\alpha = 1.85$, $\beta = 0.48$. A Palo Verde submittal to the NRC contains data relating RPC measured length to the structural length determined by destructive examination.[1] Based on evaluation of these data, the mean error for the length measurements was zero, and the standard deviation for length measurements was 0.5 inches. The POD as a function of length was approximated as being zero at 0.1 inches and 0.95 at 0.3 inches and longer, with a straight line variation between these two values. The flaw size distribution was adjusted to reflect measurement error and POD using the method described by Heasler.[2] The resulting estimated "actual" flaw size distribution is shown in Figures B-10C and B-

10D. A "detection efficiency" of 0.66 was determined by setting it equal to the integral of the probability of detection times the actual distribution divided by the integral of the actual size distribution. The integrals were taken for flaws in the range of 0.1 and 4.1 inches in length.

A distribution of estimated crack depths for freespan cracks in Palo Verde 2 is shown in Figures B-11A and B-11B. The gamma distribution parameters for the freespan crack depth distribution are: $\alpha = 11.04$, $\beta = 3.99$. Based on analysis of data scatter presented in a Palo Verde submittal to the NRC,[3] the mean error was estimated at zero and the standard deviation as 14% of wall. The POD was taken from a curve in the same submittal except that the maximum POD was set at 0.95 (reached at 68% of wall) (Figure B-11F). The flaw size distribution was adjusted to reflect measurement error and POD using the method described by Heasler.[4] To accomplish this adjustment, the standard deviation for measurement error had to be reduced to 12% of wall because the estimated 14% of wall value led to an unrealistic actual crack size distribution. The resulting estimated "actual" flaw size distribution is shown in Figures B-11C and B-11D. Note that the depth distribution indicates that there is essentially no chance of a defect being through wall. Also note that a "detection efficiency" of 0.66 was determined by setting it equal to the integral of the probability of detection times the actual distribution divided by the integral of the actual size distribution. The integrals were taken for flaws in the range of 20 to 100% of wall.

DEI performed a check of the probability of the above length and depth distributions causing a tube burst. This check was performed using Monte Carlo sampling and showed that there were no cases out of 10,000 trials where a defect had both a length over 1.8 inches and a depth over 90% of wall, i.e., no cases occurred where burst would be predicted under normal operating conditions. While this is considered reasonable for cases where extensive inspections for freespan defects are being performed, it is not considered realistic for the Wextex units being considered here, as discussed below.

The flaw size depth distribution based on the Palo Verde data is for a unit where a rupture had occurred and very thorough and detailed inspections for free span cracking are being performed. This is not the case for the Wextex plants, where no ruptures due to freespan cracks have occurred and relatively limited freespan cracking has been detected by ECT. At these plants routine bobbin coil inspections are typically relied upon for scanning for freespan defects. With this level of inspection, there exists some likelihood of short through wall flaws being present, and there probably also is some chance of burst occurring, say one per every few thousand tubes with free span defects. To reflect these possibilities (i.e., possibilities of through wall defects and very occasional ruptures) the

depth distribution was adjusted by trial and error to result in a about a 2% chance of a defect being through wall (most will be very short and thus cause negligible leakage) and about a 0.1% chance of a defect causing a burst, where burst was considered as occurring if the flaw has both a length over 1.8 inches and a depth over 90% of wall (for 3/4" diameter tubes). The depth distribution providing these results, when combined with the length distribution of Figure B-10C and 10D, is shown on Figure B-11E.

Distributing the numbers of flaws expected at the end of the operating cycle into size bins is not practical since there are two independent size distributions. The user will have to determine the probability of having a defect with both a large length and a large depth using Monte Carlo sampling or equivalent of the two distributions. Note that the total number of flaws should be increased from the numbers of detectable flaws determined above by dividing by the product of the detection efficiencies of the length and depth distributions, i.e., by dividing by 0.66 x 0.88 = 0.58 or multiplying by 1/.58 = 1.72.

---

1 Palo Verde Nuclear Generating Station Unit 2 Steam Generator Evaluation, August 1995, in NRC PDR, 9509120077 950907, Docket No. 50-529.

2 P. G. Heasler, et al., Analysis Before Test: Estimation of Fabrication Defect Rates in Reactor Pressure Vessels, Draft PNL report for NRC, Nov. 1994.

3 Palo Verde Nuclear Generating Station Unit 2 Steam Generator Evaluation, August 1995, in NRC PDR, 9509120077 950907, Docket No. 50-529.

4 P. G. Heasler, et al., Analysis Before Test: Estimation of Fabrication Defect Rates in Reactor Pressure Vessels, Draft PNL report for NRC, Nov. 1994.

Figure A-17. Industry Time to Detect Freespan IGA/SCC - Median Rank Analysis - All Domestic Westinghouse Design Model 51 Plants - Thot >= 600 deg F

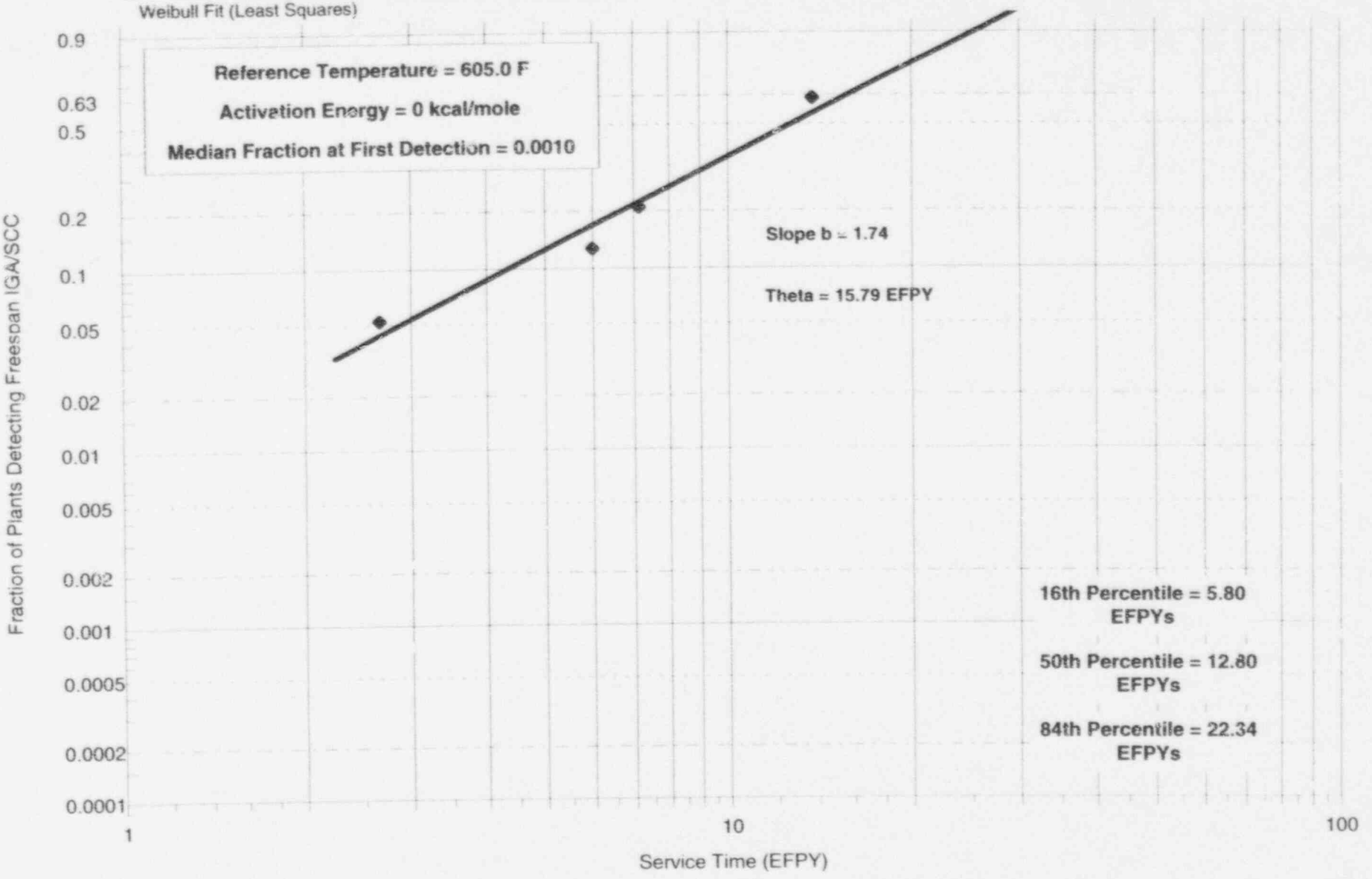

Figure A-16A. Weibull Slopes for Freespan IGA/SCC in Westinghouse Preheater LTMA Plants

No. Plants = 7

Median Slope = 2.93
16% Slope = 2.33
84% Slope = 3.70

No.	Plant	Slope b	Median Rank	Comment
1	A	2.19	0.095	Cycles 8 through 10 for tubes repaired due to freespan IGA/SCC
2	B	2.48	0.230	Cycles 8B through 10 for tubes repaired due to freespan IGA/SCC
3	C	2.86	0.365	Cycle 8 for tubes repaired due to freespan IGA/SCC
4	D	2.93	0.500	Cycles 6 through 10 for tubes repaired due to freespan defects
5	E	3.46	0.635	Cycles 6 through 8 for tubes repaired due to freespan defects
6	F	3.67	0.770	Cycles 5B and 6 for tubes repaired due to freespan IGA/SCC
7	G	3.93	0.905	Cycles 5 and 6 for tubes repaired due to freespan IGA/SCC

Updated: Aug-96

Dominion Engineering, Inc.

Figure A-16B. Weibull Fit to Preheater Freespan Slopes

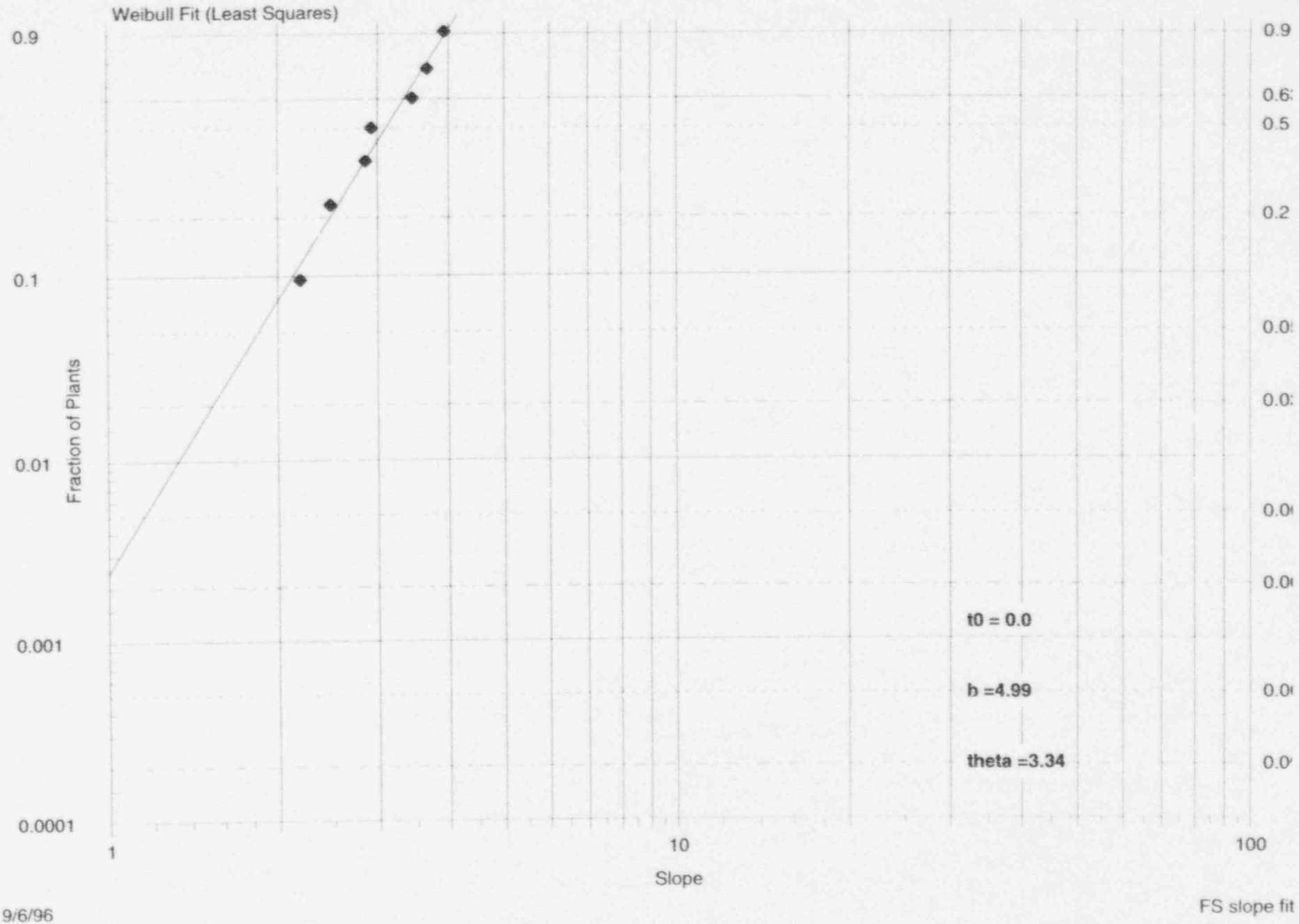

9/6/96

Figure C-8. Weibull Distribution Monte Carlo - Free Span Cracks

Distributions

Slope	b	Time to 0.100% Failures	t0%	Susceptible Fraction	ß	
Type [1]	Weibull	Type [1]	Weibull	Type [1]		
Slope	4.99	Slope	1.74	ß	1	
Theta	3.34	Theta	15.79		10	
		error				
		error				
Min b	1	Min t0%	0.00	Min ß	0.001	
Max b	8	Max t0%	6850.1	Max ß	1	
Normalization	1.00	Normalization	1.00	Normalization		
Start Trunc	0.0024	Start Trunc	0.0000	Start Trunc		

Times of Interest

14.0	EFPY
15.2	EFPY

Results
(1000 trials)

Median Delta F	16%ile Delta F	84%ile Delta F
0.000342	0.000068	0.00409

Figure C-9. Freespan Delta F Runs

	Median Delta F	16%ile Delta F	84%ile Delta F
	0.000323	0.000069	0.00357
	0.000360	0.000065	0.00341
	0.000325	0.000072	0.00390
	0.000277	0.000060	0.00256
	0.000320	0.000065	0.00356
mean	0.000321	0.000066	0.00340
delta N	3.3	0.7	34.6

Figure B-10A. Palo Verde 2 Free Span Defect Length

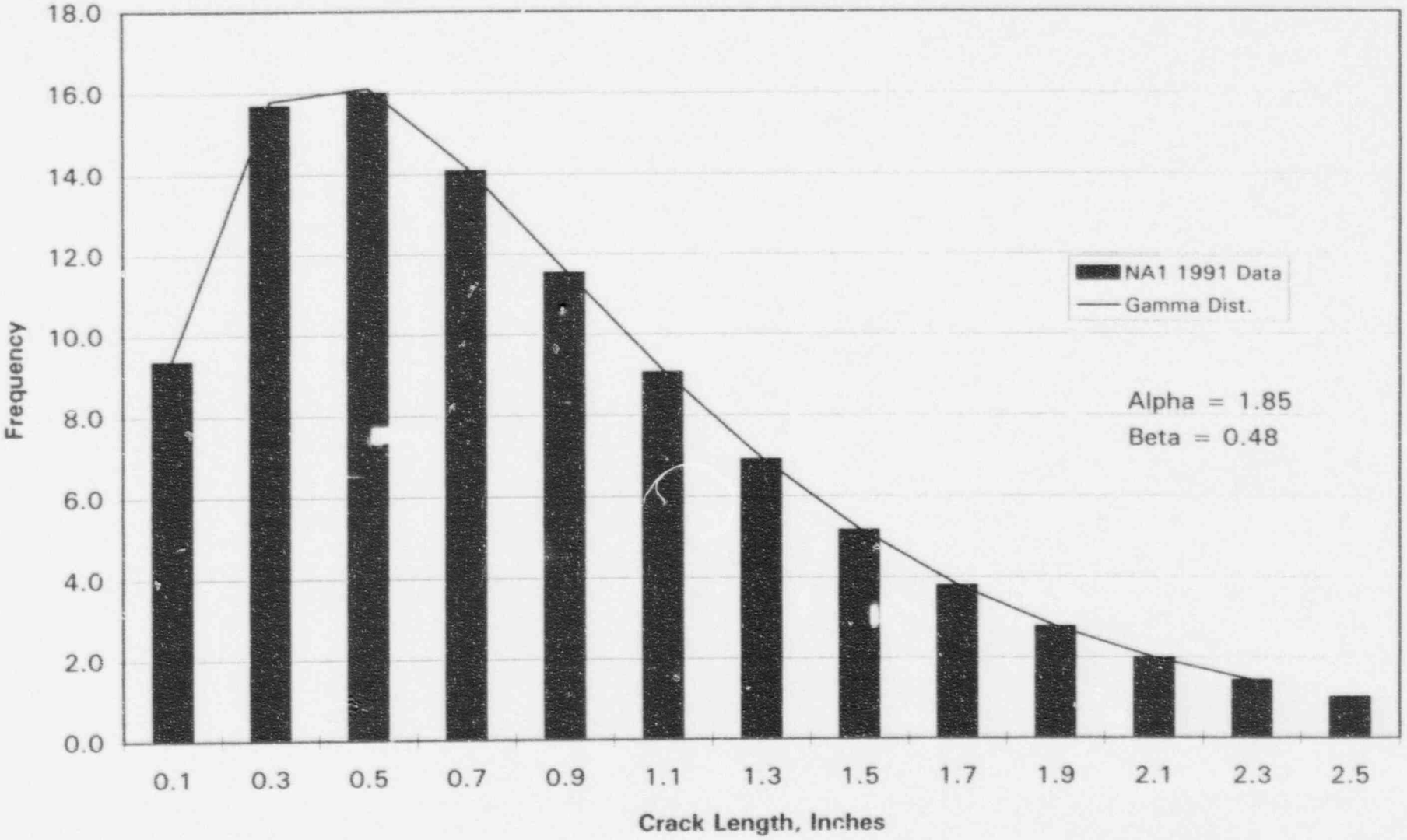

Figure B-10B. Palo Verde 2 Free Span Defect Length

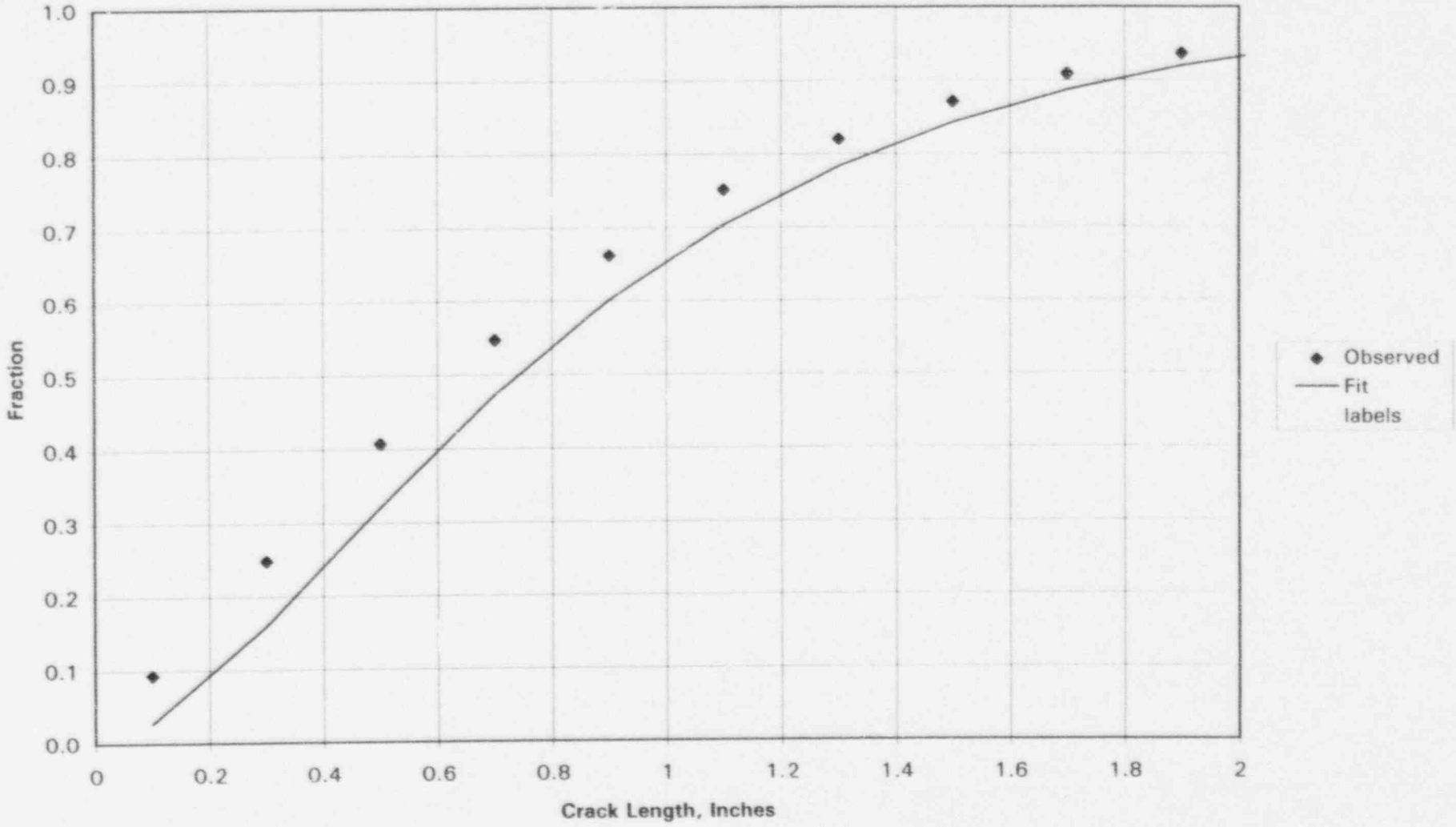

Figure B-10C. Free Span Defect Length

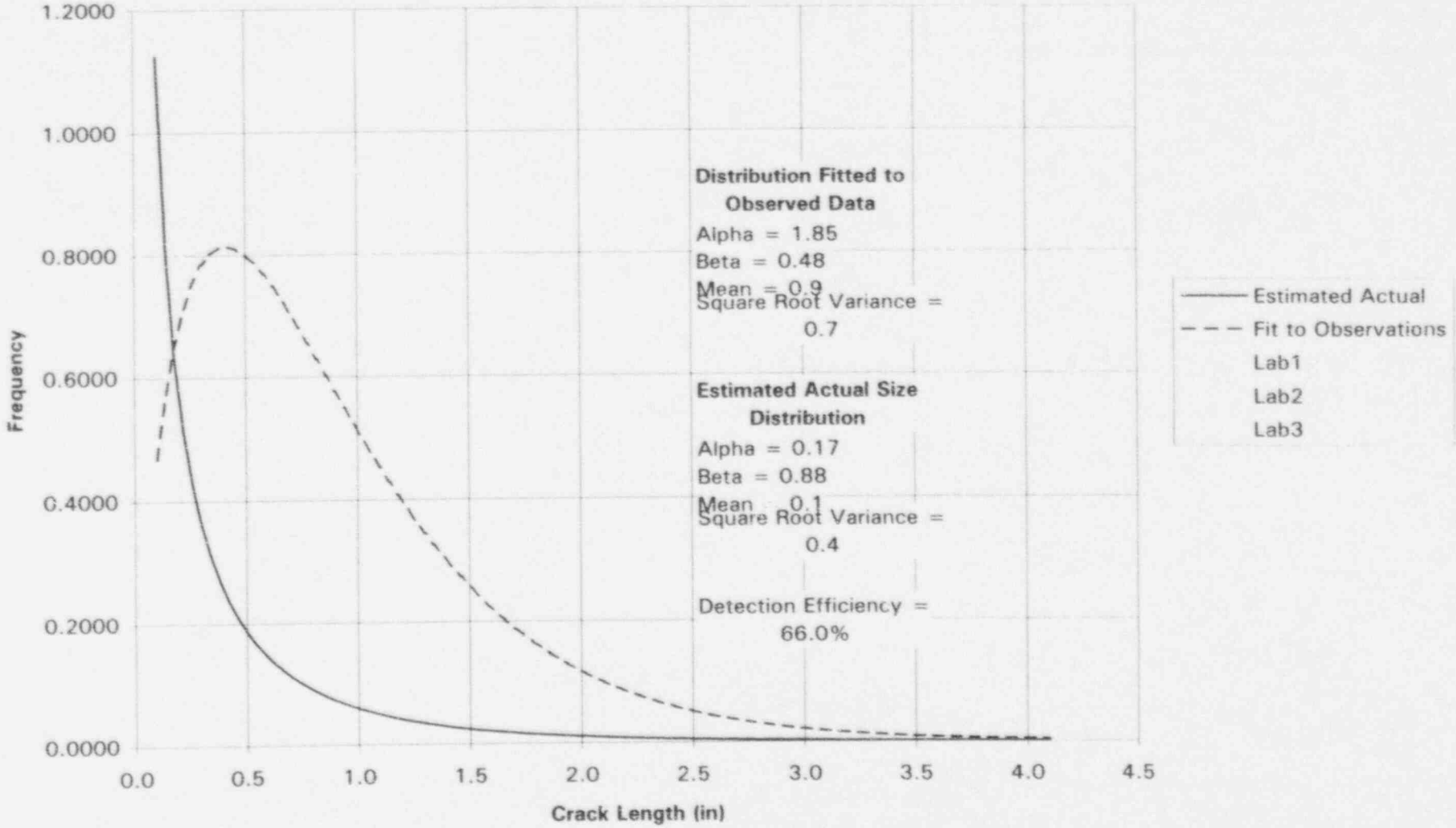

Figure B-10D. Free Span Defect Length

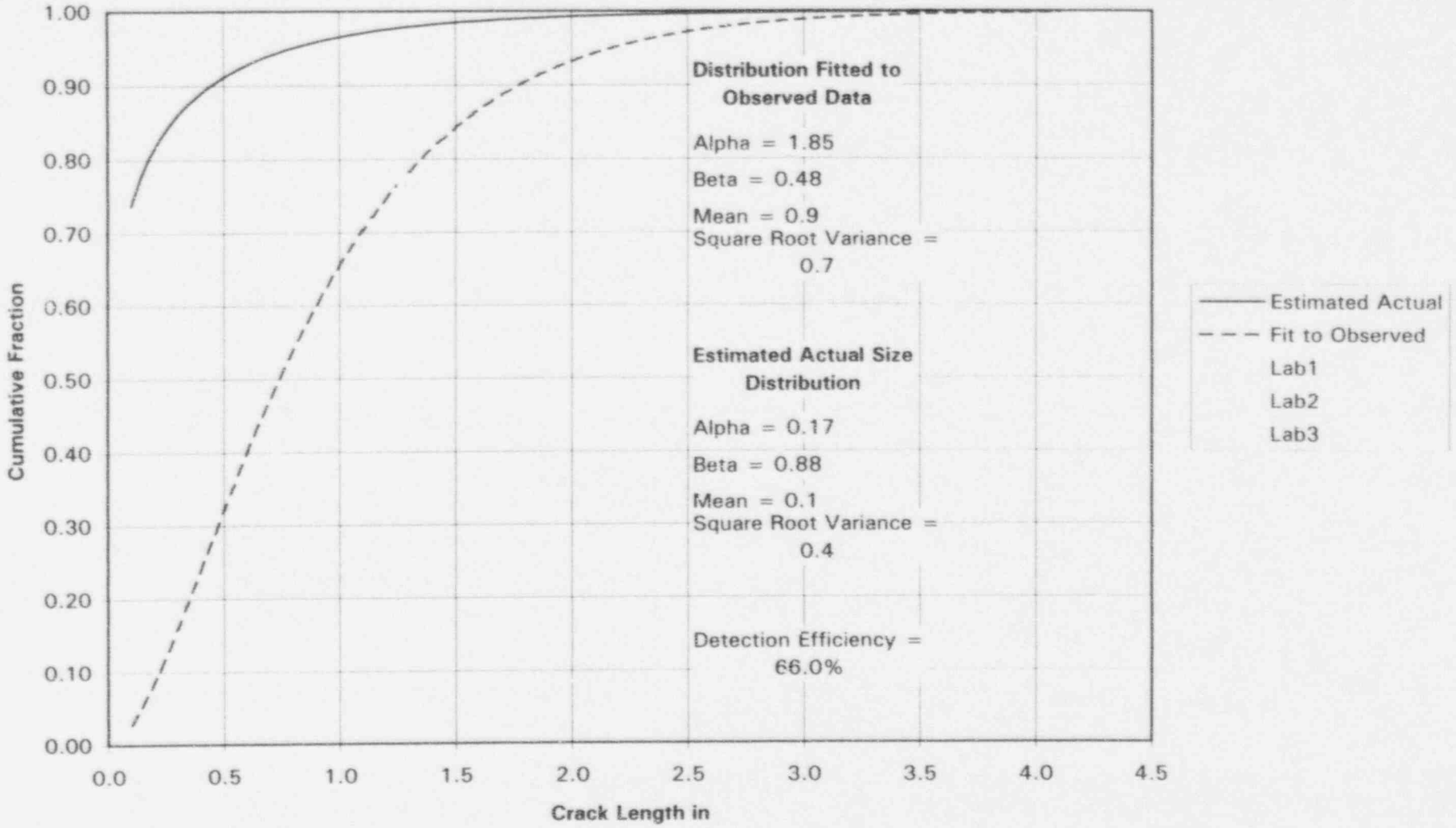

Figure B-11A. PV 2 Free Span Defect Depths

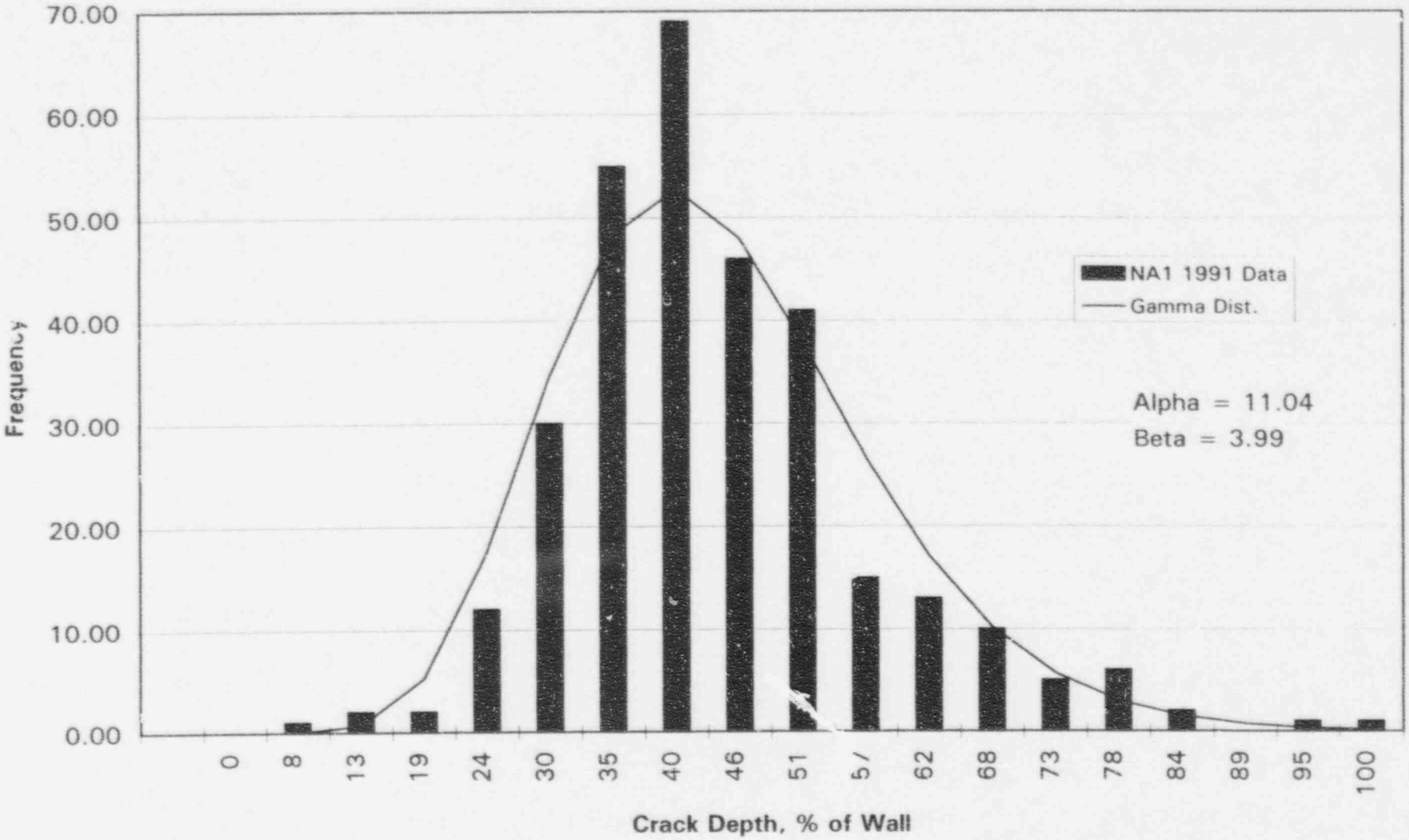

Figure B-11B. PV 2 Free Span Defect Depths

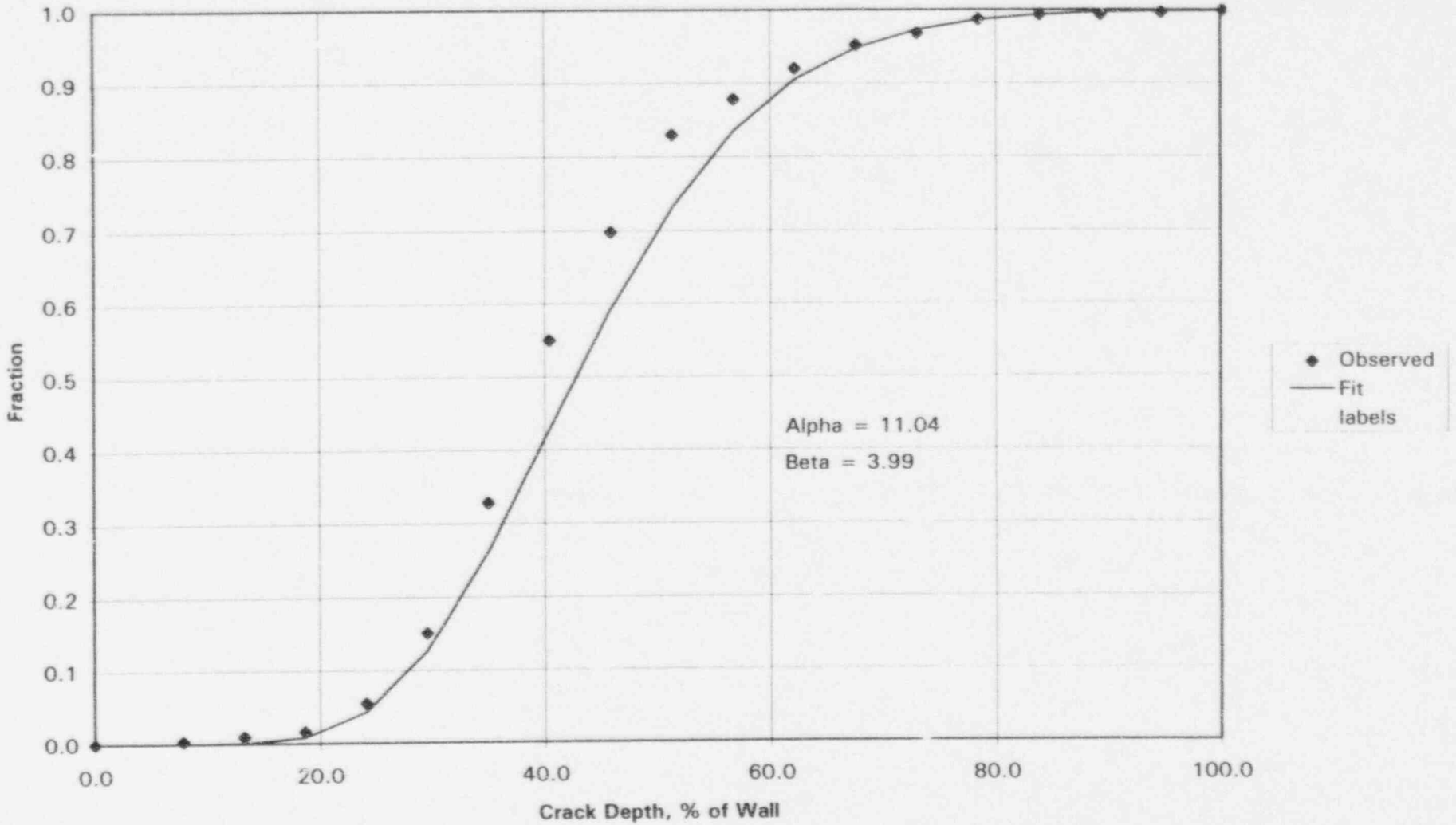

Figure B-11C. Free Span Defect Depths

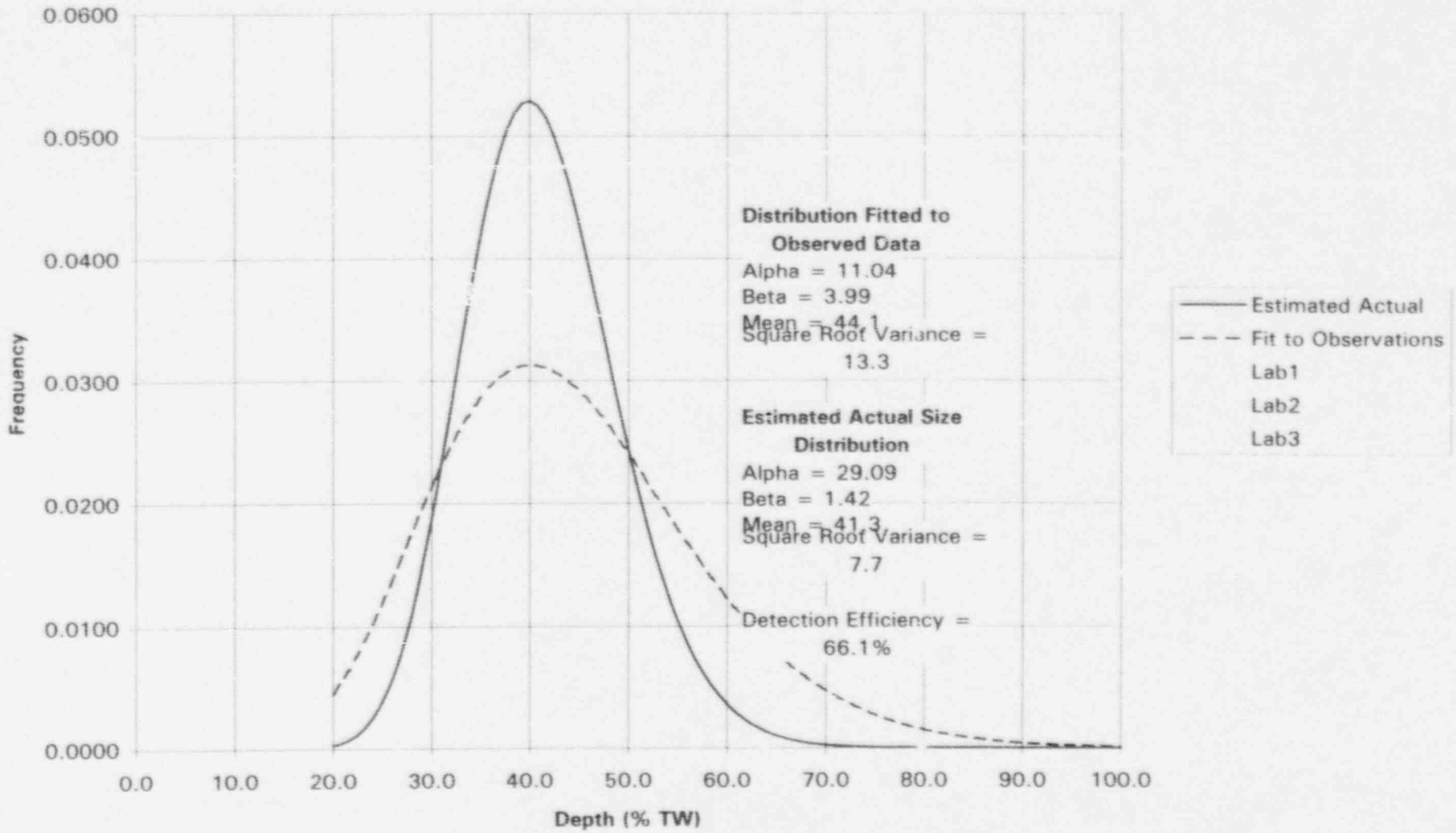

Figure B-11D. Free Span Defect Depths

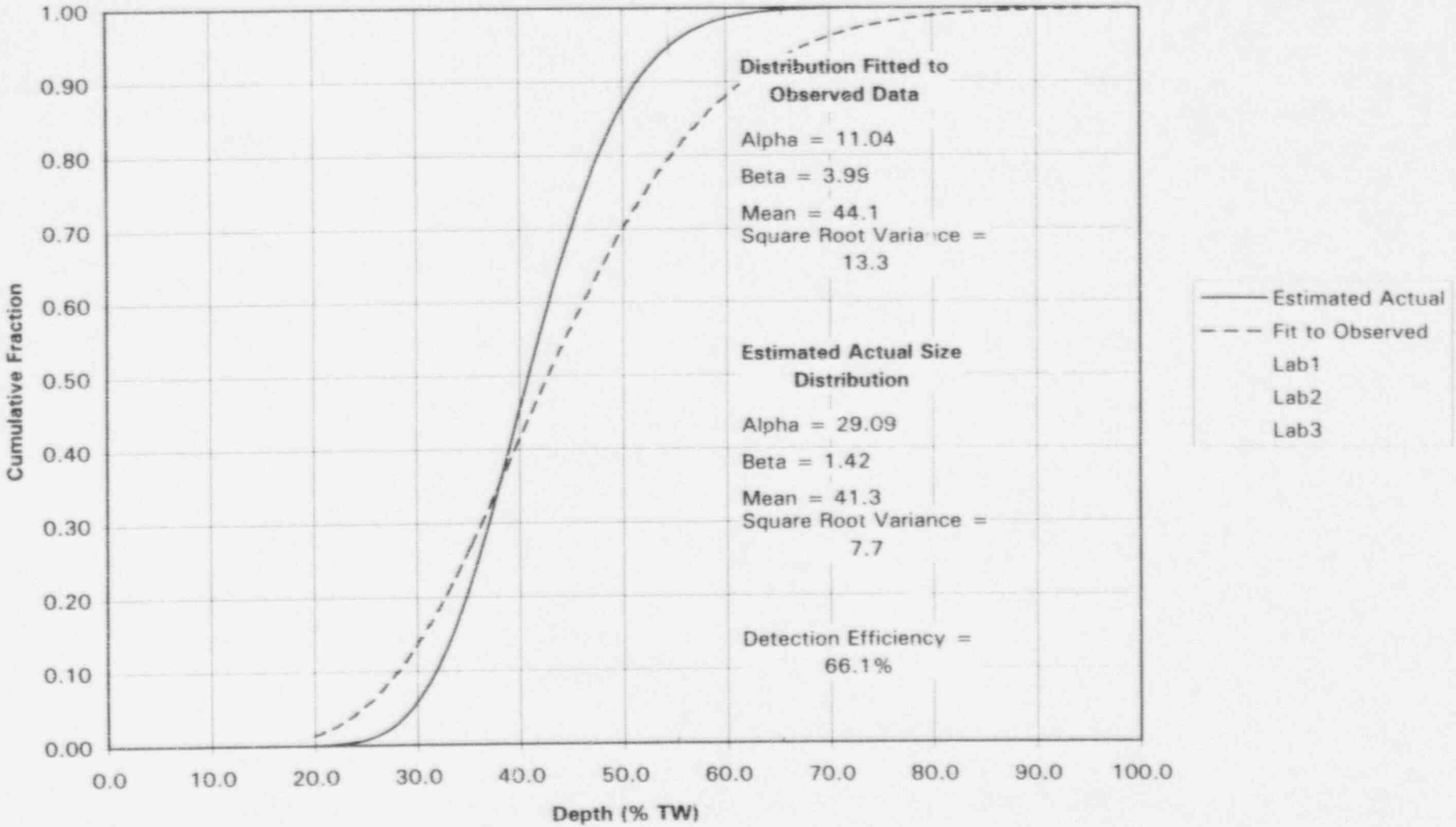

Figure B-11E. Cumulative Depth Distribution for Free Span Cracks

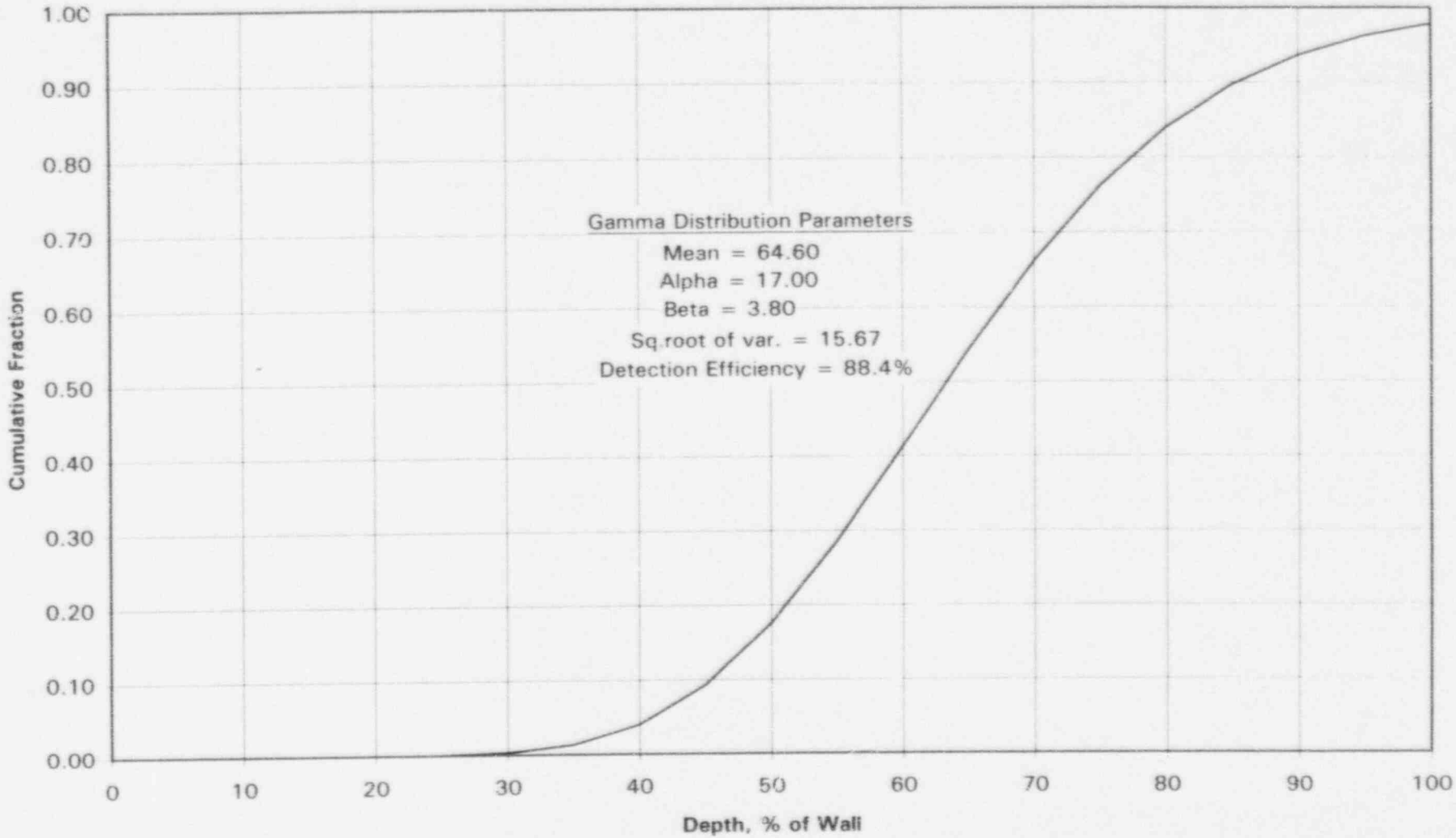

Figure B-11F. Axial Free Span Defects - Probability of Detection

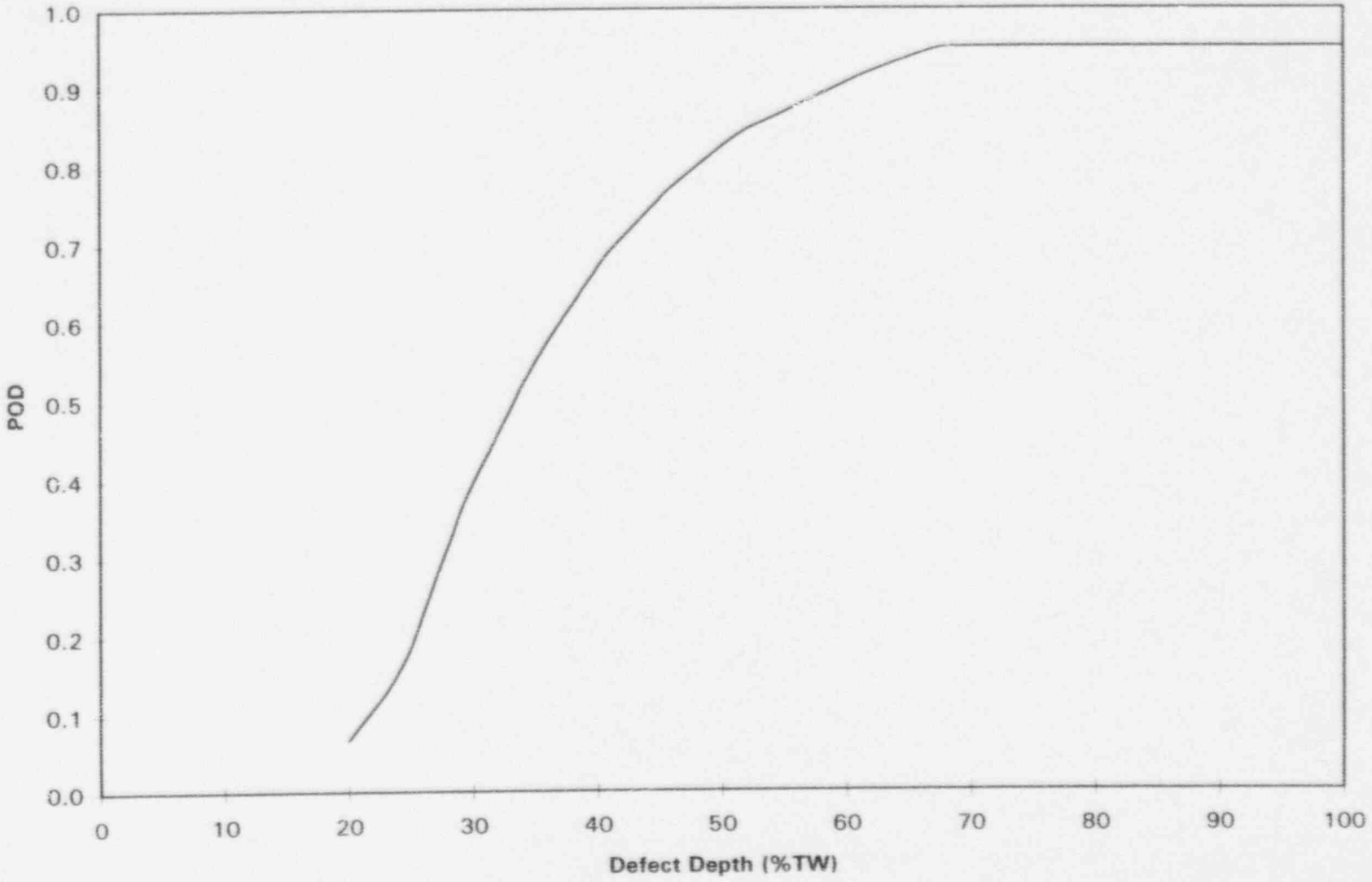

4. Sludge Pile IGA/SCC

The distribution of times to 1% cracking of free span SCC for Westinghouse feedring steam generators for a hot leg temperature of 605°F is shown on Figure A-22 (median time of 14.7 EFPY, 16th percentile time of 10.9 EFPY and 84th percentile time of 18.2 EFPY). The Weibull slopes for sludge pile IGA/SCC are listed on Figure A-23A, and a Weibull fit to the slopes is shown on Figure A-23B (fitted median of about 3.4). The distributions for intercept times and slopes were used in a Monte Carlo evaluation of the type described in Section 5 to determine a distribution of the numbers of newly detectable flaws that develop during the operating cycle, i.e., between 14.0 and 15.2 EFPY. A typical run for the Monte Carlo evaluation is shown on Figure C-10. Results of five runs, representing 5000 trials, are shown on Figure C-11. Figure C-11 shows median, 16th percentile and 84th percentile results for both fractions and numbers of tubes. These are taken as representing moderately affected, lightly affected and severely affected units respectively. The results for the three cases are as follows:

Case	Delta F	Number of Tubes with Detectable
	%	Flaws at 15.2 EFPY
Moderate	0.22	23
Severe	0.89	90
Light	0.10	11

As discussed in Appendix B, distributions for sludge pile IGA/SCC are taken to be the same as for freespan SCC. Crack distributions for freespan cracking are covered in the previous section. Gamma distributions for flaw length are shown on Figures B-10C and B-10D, and for flaw depth are shown on Figure B-11E. The detection efficiencies of 0.66 determined for the length distribution of freespan flaws and of 0.88 for the depth distribution of freespan flaws likewise apply.

Distributing the numbers of flaws expected at the end of the operating cycle into size bins is not practical since there are two independent size distributions. The user will have to determine the probability of having a defect with both a large length and a large depth using Monte Carlo sampling or equivalent of the two distributions.

Note that the total number of flaws should be increased from the numbers of detectable flaws determined above by dividing by the product of the detection efficiencies of the length and depth distributions, i.e., by dividing by 0.66 x 0.88 = 0.58 or multiplying by 1/.58 = 1.72.

Figure A-22. Industry Average Time to 1% HL SP IGA/SCC - Median Rank Analysis - West. Feedring Plants with FDE and no FDBs

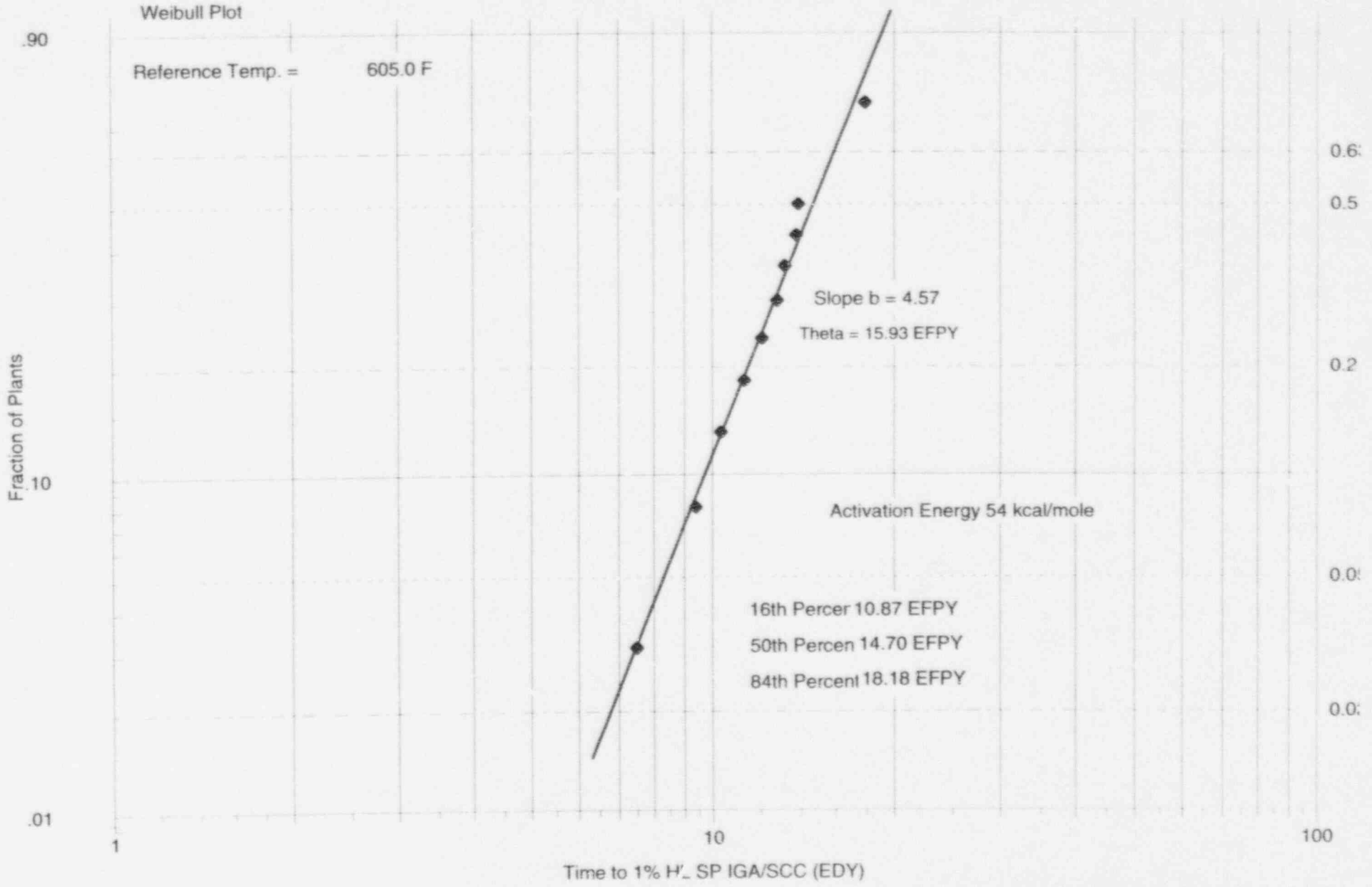

Figure A-23A. Weibull Slopes for HL SP IGA/SCC - LTMA 600

No. Plants = 18

Median Slope = 4.02
16% Slope = 1.07
84% Slope = 6.62

No.	Plant	Slope b	Median Rank	Comment
1	A	0.41	0.038	
2	B	0.89	0.092	
3	C	1.02	0.147	
4	D	1.21	0.201	
5	E	1.33	0.255	
6	F	1.74	0.310	
7	G	2.43	0.364	
8	H	3.27	0.418	
9	I	3.87	0.473	
10	J	4.16	0.527	
11	K	4.23	0.582	
12	L	4.58	0.636	
13	M	4.76	0.690	
14	N	4.81	0.745	
15	O	6.30	0.799	
16	P	6.72	0.853	
17	Q	7.61	0.908	
18	R	14.60	0.962	

Updated: Aug-96

Dominion Engineering, Inc.

Figure A-23B. Weibull Fit to Sludge Pile IGA/SCC Slopes

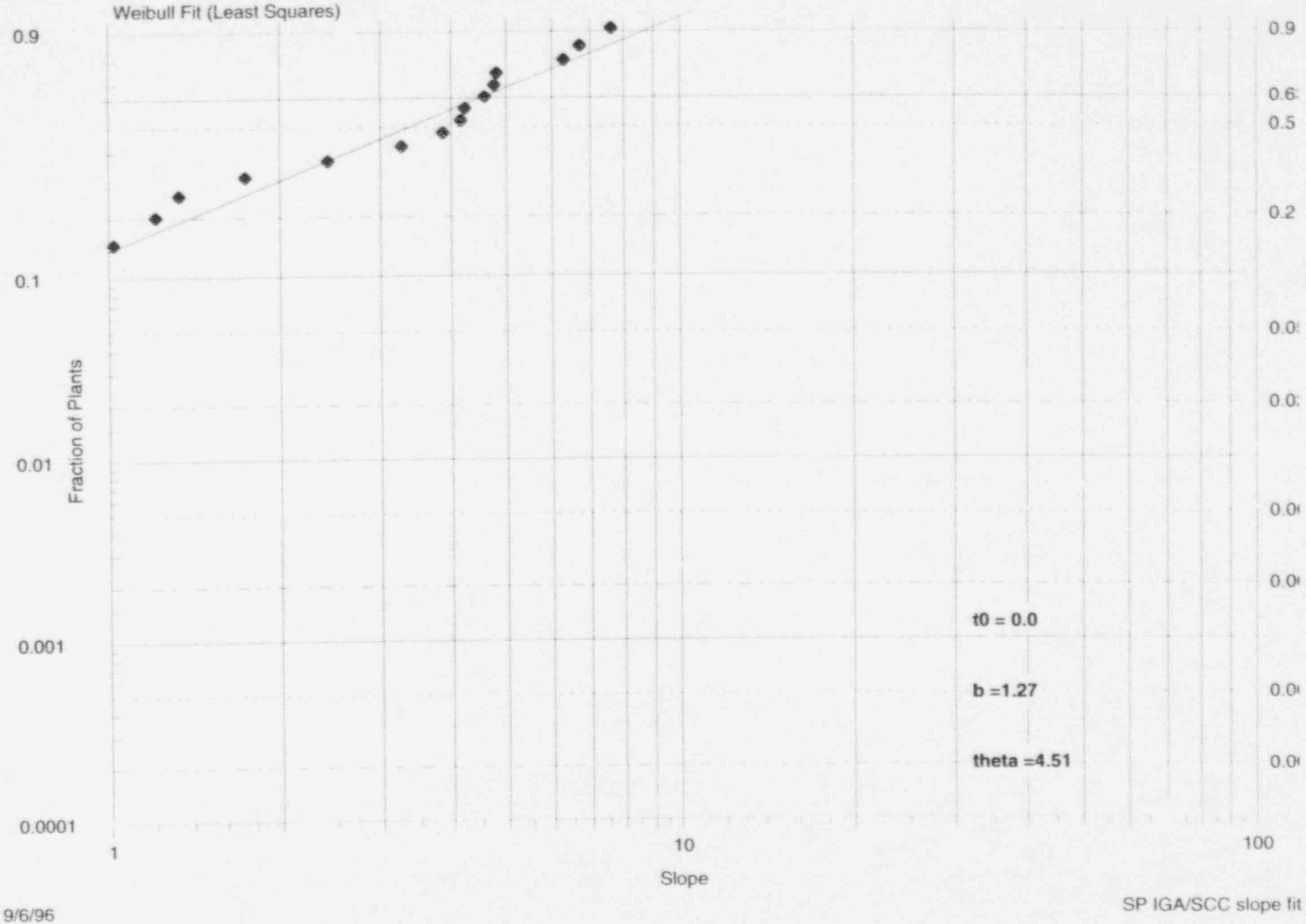

9/6/96

Figure C-10. Weibull Distribution Monte Carlo - Sludge Pile IGA/SCC

Distributions

Slope	b	Time to 1.000% Failures	t1%	Susceptible Fraction	ß		
Type [1]	Weibull	Type [1]	Weibull	Type [1]			
Slope	1.27	Slope	4.57	ß	1		
Theta	4.51	Theta	15.93		10		
		error					
		error					
Min b	1	Min t1%	0.00	Min ß	0.001		
Max b	8	Max t1%	18474.1	Max ß	1		
Normalization	1.36	Normalization	1.00	Normalization			
Start Trunc	0.1373	Start Trunc	0.0000	Start Trunc			

Times of Interest

14.0	EFPY
15.2	EFPY

Results
(1000 trials)

Median Delta F	16%ile Delta F	84%ile Delta F
0.002069	0.000984	0.00839

Figure C-11. Sludge Pile IGA/SCC Delta F Runs

	Median Delta F	16%ile Delta F	84%ile Delta F
	0.002199	0.001024	0.01045
	0.002221	0.001079	0.00841
	0.002306	0.001077	0.00800
	0.002386	0.001023	0.00862
	0.002060	0.001022	0.00886
mean	0.002234	0.001045	0.00887
delta N	22.7	10.6	90.1

5. Axial ODSCC at TSPs (non dented)

Evaluation of this mode needs to account for the fact that data for development of these flaws is mainly for flaws that were repairable using the older 40% of wall plugging criterion, while current practice is to repair in accordance with 2-volt alternate repair criteria (ARC). To accommodate this situation the numbers of tubes with detectable indications using the older 40% of wall criterion is first determined, and then the number of tubes removed from service as a result of plugging will be estimated.

The distribution of times to 1% of tubes with detectable axial ODSCC at TSPs for Westinghouse feedring steam generators for a hot leg temperature of 605°F is shown on Figure A-20 (median time of 13.4 EFPY, 16th percentile time of 7.49 EFPY and 84th percentile time of 20.2 EFPY). Per Appendix A, this value is for pluggable flaws using a 40% of wall criterion, with bobbin coil (BC) voltage of about 0.85 or higher. The Weibull slopes for these units are listed on Figure A-21A, and a Weibull fit to the slopes is shown on Figure A-21B (fitted median of about 4.5). The distributions for intercept times and slopes were used in a Monte Carlo evaluation of the type described in Section 5 to determine a distribution of the numbers of detectable flaws that have developed at 15.2 EFPY (some of these flaws will have been removed because of large voltage signals, as discussed later). A typical run for the Monte Carlo evaluation is shown on Figure C-12. Results of five runs, representing 5000 trials, are shown on Figure C-13. Figure C-13 shows median, 16th percentile and 84th percentile results for both fractions and numbers of tubes. These are taken as representing moderately affected, lightly affected and severely affected units respectively. The results for the three cases are as follows:

Case	F %	Number of Tubes with Detectable Flaws at 15.2 EFPY*
Moderate	1.49	151
Severe	15.4	1568
Light	0.32	33

* Includes repaired tubes.

Over time, the voltages of tubes with ODSCC tend to increase at an average rate of about 0.2 volts per EFPY. A relatively high fraction of tubes with voltages over the 2 volt plugging criteria are usually confirmed by RPC and thus require repair. After one or two more cycles, this fraction is expected to reach essentially 100%. To simplify the calculation for tubes repaired, it is therefore assumed that all tubes require repair when their voltage reaches 2.2 volts. With this assumption, tubes typically require repair at (2.2 - 0.85)/0.2 = 6.75 EFPY after reaching 0.85 volts. Using this value, tubes that developed detectable flaws at the 0.85 volt level at 14.0 - 6.75 = 7.25 EFPY or earlier are likely to have developed voltages high enough to result in plugging by 14.0 EFPY. Monte Carlo evaluations similar to those described above were performed to determine these values, with the results shown in Figures C-14 and 15. These values were then subtracted from those of the 15.2 EFPY case to determine the number of tubes with detectable flaws in service at 15.2 EFPY, as follows:

Case	Number of Tubes with Detectable Flaws at 15.2 EFPY	Number of Tubes with Detectable Flaws at 7.25 EFPY, and Plugged by 14.0 EFPY	Number of In-Service Tubes with Detectable Flaws at 15.2 EFPY
Moderate	151	12	139
Severe	1568	98	1470
Light	33	1	32

As discussed in Appendix B, a crack size distribution for this mode of cracking at Farley 1 is taken as being typical. Figure B-13A shows a crack size distribution developed from voltage data for a recent Farley inspection, for assumed 0.75 inch long cracks. A correlation between field bobbin coil voltages and the depth of 0.75 inch long cracks was developed using burst pressure - voltage data for pulled tubes to estimate the burst pressure as a function of signal voltage, and then using the ANL failure pressure correlation to convert these burst pressures to the depths of 0.75 inch long cracks. Based on evaluation of these data, the mean error for the depth measurements was zero, and the standard deviation was 15% of wall. The POD as a function of depth was approximated as being zero at zero defect depth and increasing linearly until it became tangent with the POD curve for freespan defects discussed in Section 3 (a POD of 0.71 at a depth of 40%); the resulting curve is shown in Figure B-13E. The reason for running the POD all the way to zero is to allow treatment of the numerous equivalent cracks of shallow depths shown in Figure B-13A. The presence

of the shallow cracks is a result of assuming that all cracks are 0.75 inches long. In actual fact, many small voltage signals are for shorter cracks that are deep enough to be detected. The flaw size distribution was adjusted to reflect measurement error and POD using the method described by Heasler.[1] To accomplish this adjustment, the standard deviation for measurement error had to be reduced to 5% of wall because the estimated 15% of wall value led to an unrealistic actual crack size distribution. The resulting estimated "actual" flaw size distribution is shown in Figures B-13C and B-13D. A "detection efficiency" of 0.244 was determined by setting it equal to the integral of the probability of detection times the actual distribution divided by the integral of the actual size distribution. The integrals were taken for flaws over 10% of wall in depth.

The numbers of unrepaired flaws expected at the end of the operating cycle, i.e., at 15.2 EFPY, were then distributed in size using the actual flaw size distribution of Figures B-13C and B-13D. The results of this distribution are shown in Figure C-16. Note that the total number of flaws was increased from the predicted number of detectable flaws using the efficiency factor determined above.

P. G. Heasler, et al., Analysis Before Test: Estimation of Fabrication Defect Rates in Reactor Pressure Vessels, Draft PNL report for NRC, Nov. 1994.

Figure A-20. Industry Time to 1% HL TSP IGA/SCC - Median Rank Analysis - All Westinghouse Design LTMA Drilled Hole Feedring Plants - No Prior Phosphate

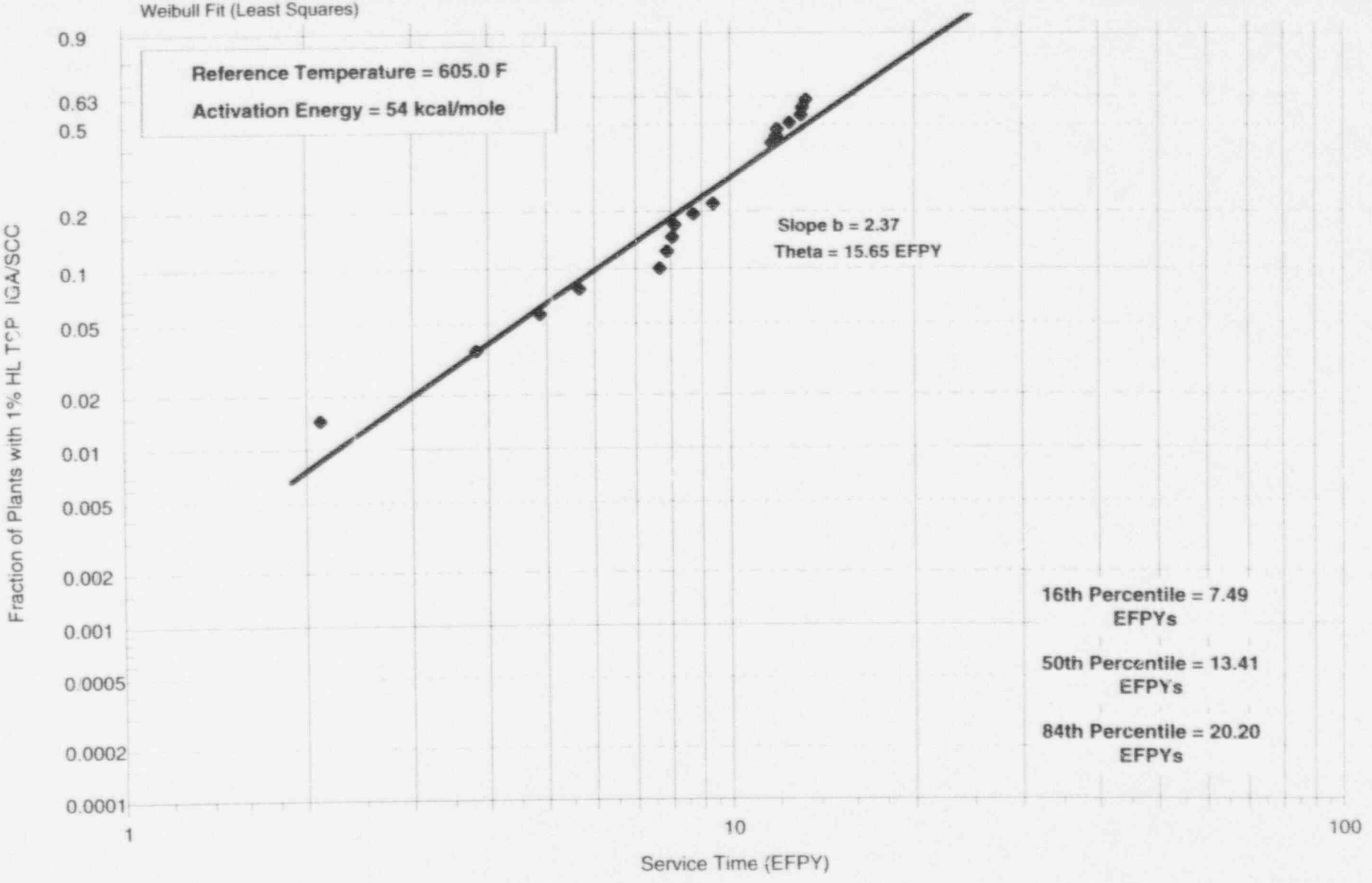

Figure A-21A. Weibull Slopes for HL TSP IGA/SCC in Westinghouse Feedring LTMA Plants Using Latest WC
(Plants with greater than 1% tubes affected only)

No. Plants = 9

Median Slope = 3.41
16% Slope = 2.64
84% Slope = 9.15

No.	Plant	Slope b	Median Rank	Comment
1	A	2.34	0.074	Cycles 6 through 12 for all repairable defects (includes pre- and post- boric acid)
2	B	2.71	0.181	Last 8 cycles for all repairable defects (includes pre- and post- boric acid)
3	C	3.24	0.287	Cycles 13 and 14 for all BC indications
4	D	3.26	0.394	Cycle 12 for BC indications >1volt
5	E	3.41	0.500	Cycles 6 through 12 for all repairable defects (includes pre- and post- boric acid)
6	F	4.22	0.606	Cycles 9 and 10 for BC indications >1volt
7	G	4.31	0.713	Cycles 7 through 10 for all repairable defects using reanalyzed data assuming no IPC
8	H	8.75	0.819	Cycle 15 for BC tubes affected (Cycle 16 excluded)
9	I	10.81	0.926	Last 3 cycles for all repairable defects

Updated: Aug-96

Dominion Engineering, Inc.

Figure A-21B. Weibull Fit to HL TSP IGA/SCC Slopes

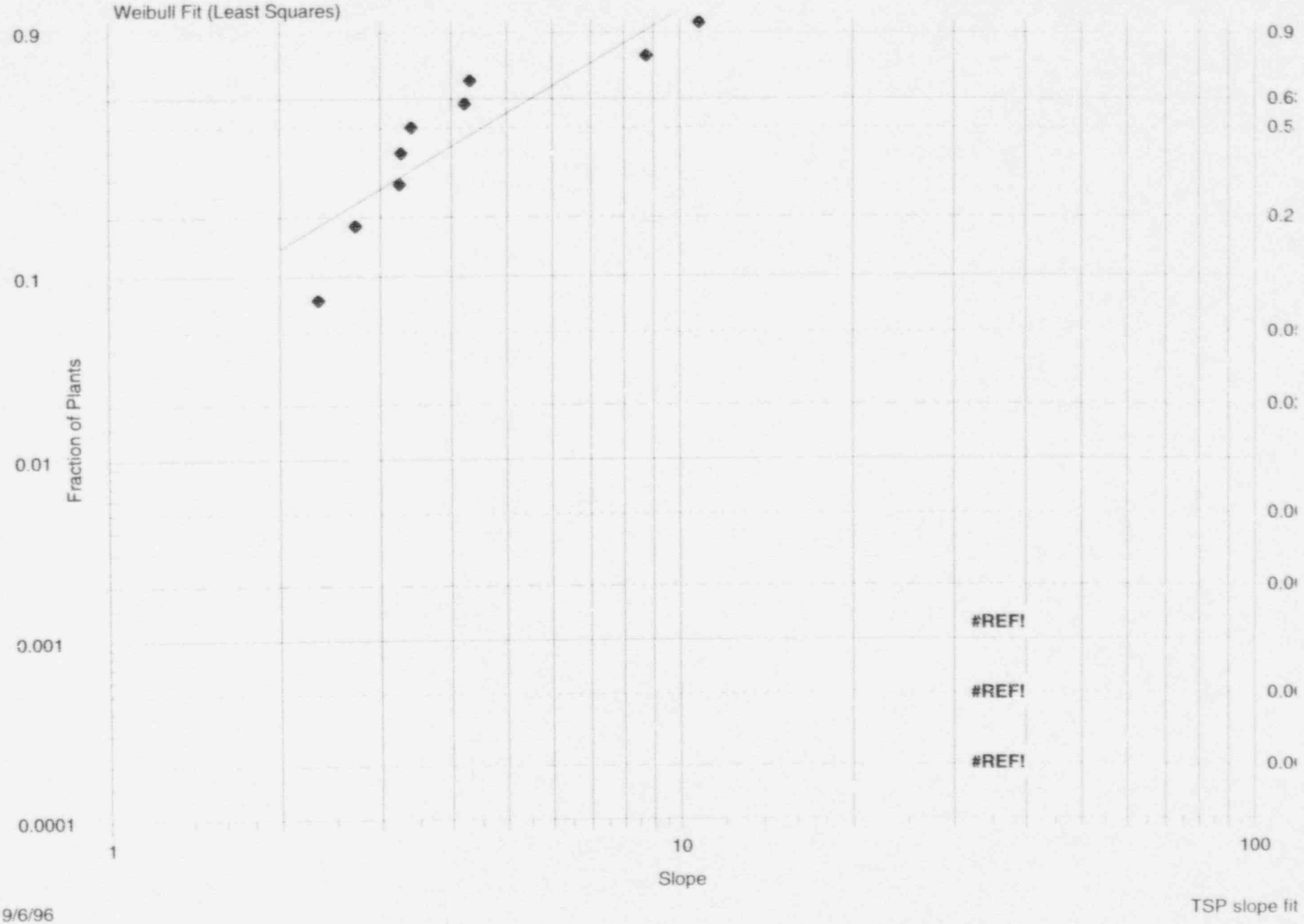

9/6/96

Figure C-12. Weibull Distribution Monte Carlo - Axial ODSCC at TSPs at 15.2 EFPY

Distributions

Slope	b		Time to 1.000% Failures	t1%	Susceptible Fraction	ß	
Type [1]	Weibull		Type [1]	Weibull	Type [1]		
Slope	1.88		Slope	2.37	ß	1	
Theta	5.52		Theta	15.65		10	
			error				
			error				
Min b	1		Min t1%	0.00	Min ß	0.001	
Max b	8		Max t1%	9084.3	Max ß	1	
Normalization	1.21		Normalization	1.00	Normalization		
Start Trunc	0.0395		Start Trunc	0.0000	Start Trunc		

Times of Interest

0.0	EFPY
15.2	EFPY

Results
(1000 trials)

Median	16%ile	84%ile
Delta F	Delta F	Delta F
0.015250	0.003091	0.12065

Figure C-13. HL TSP ODSCC 15.2 EFPY F Runs

	Median Delta F	16%ile Delta F	84%ile Delta F
	0.013685	0.003322	0.13613
	0.014797	0.003092	0.16142
	0.014207	0.003123	0.13901
	0.015874	0.003207	0.15420
	0.015896	0.003483	0.18080
mean	0.014892	0.003245	0.15431
delta N	151.4	33.0	1568.4

Figure C-14. Weibull Distribution Monte Carlo - Axial ODSCC at TSPs at 7.25 EFPY

Distributions

Slope	b	Time to 1.000% Failures	t1%	Susceptible Fraction	ß		
Type [1]	Weibull	Type [1]	Weibull	Type [1]			
Slope	1.88	Slope	2.37	ß	1		
Theta	5.52	Theta	15.65		10		
		error					
		error					
Min b	1	Min t1%	0.00	Min ß	0.001		
Max b	8	Max t1%	9084.3	Max ß	1		
Normalization	1.21	Normalization	1.00	Normalization			
Start Trunc	0.0395	Start Trunc	0.0000	Start Trunc			

Times of Interest

0.0	EFPY
7.25	EFPY

Results
(1000 trials)

Median	16%ile	84%ile
Delta F	Delta F	Delta F
0.001205	0.000099	0.00953

Figure C-15. HL TSP ODSCC 7.25 EFPY F Runs

	Median Delta F	16%ile Delta F	84%ile Delta F
	0.001164	0.000073	0.00825
	0.001237	0.000080	0.01085
	0.001151	0.000084	0.00868
	0.001126	0.000091	0.00876
	0.001383	0.000075	0.01174
mean	0.001212	0.000081	0.00965
delta N	12.3	0.8	98.1

Figure B-13A. Farley 1 1995 - Estimated Crack Depth Due to Axial ODSCC at TSPs

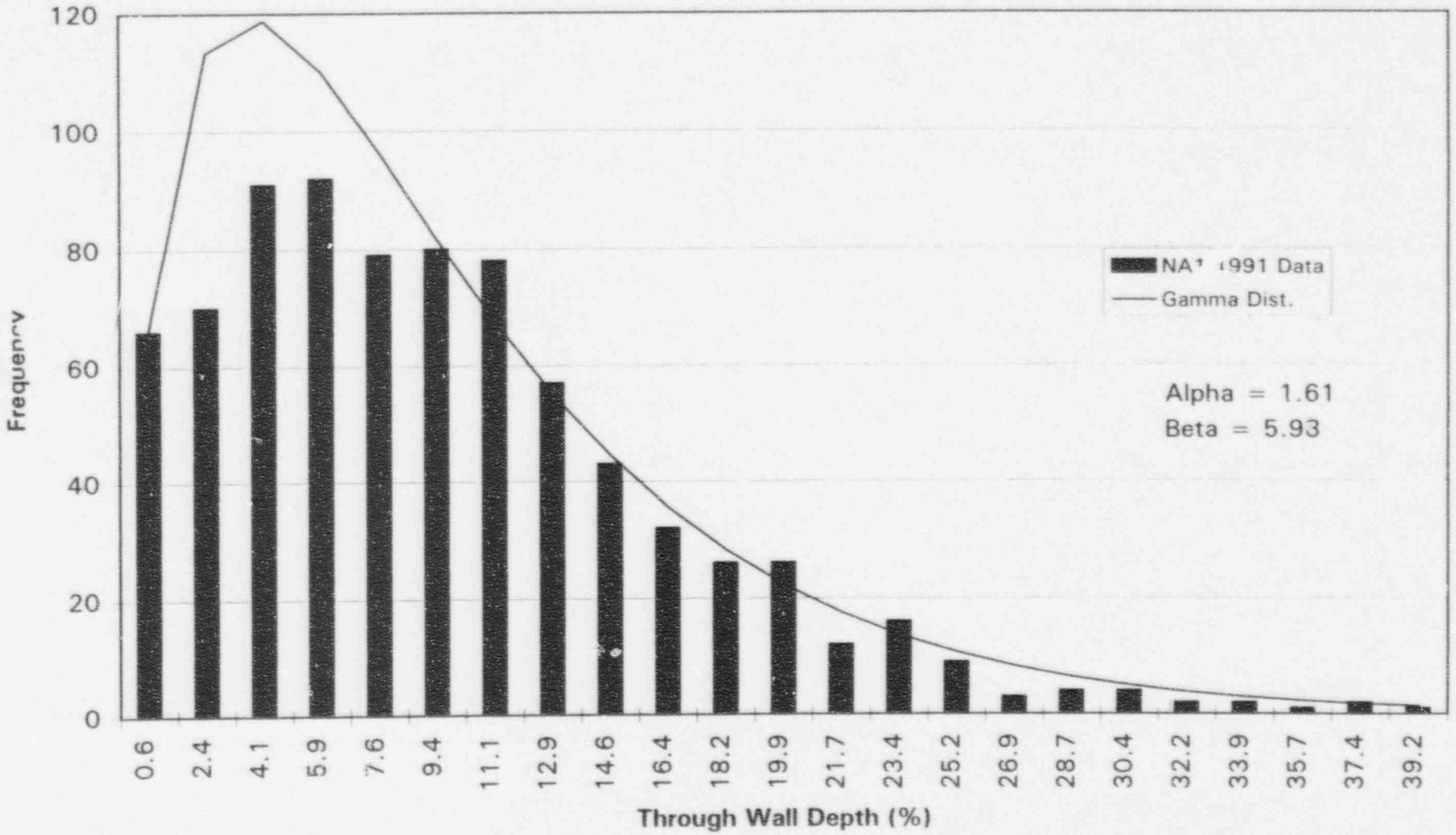

Figure B-13B. Farley 1 1995 - Estimated Crack Depth Due to Axial ODSCC at TSPs

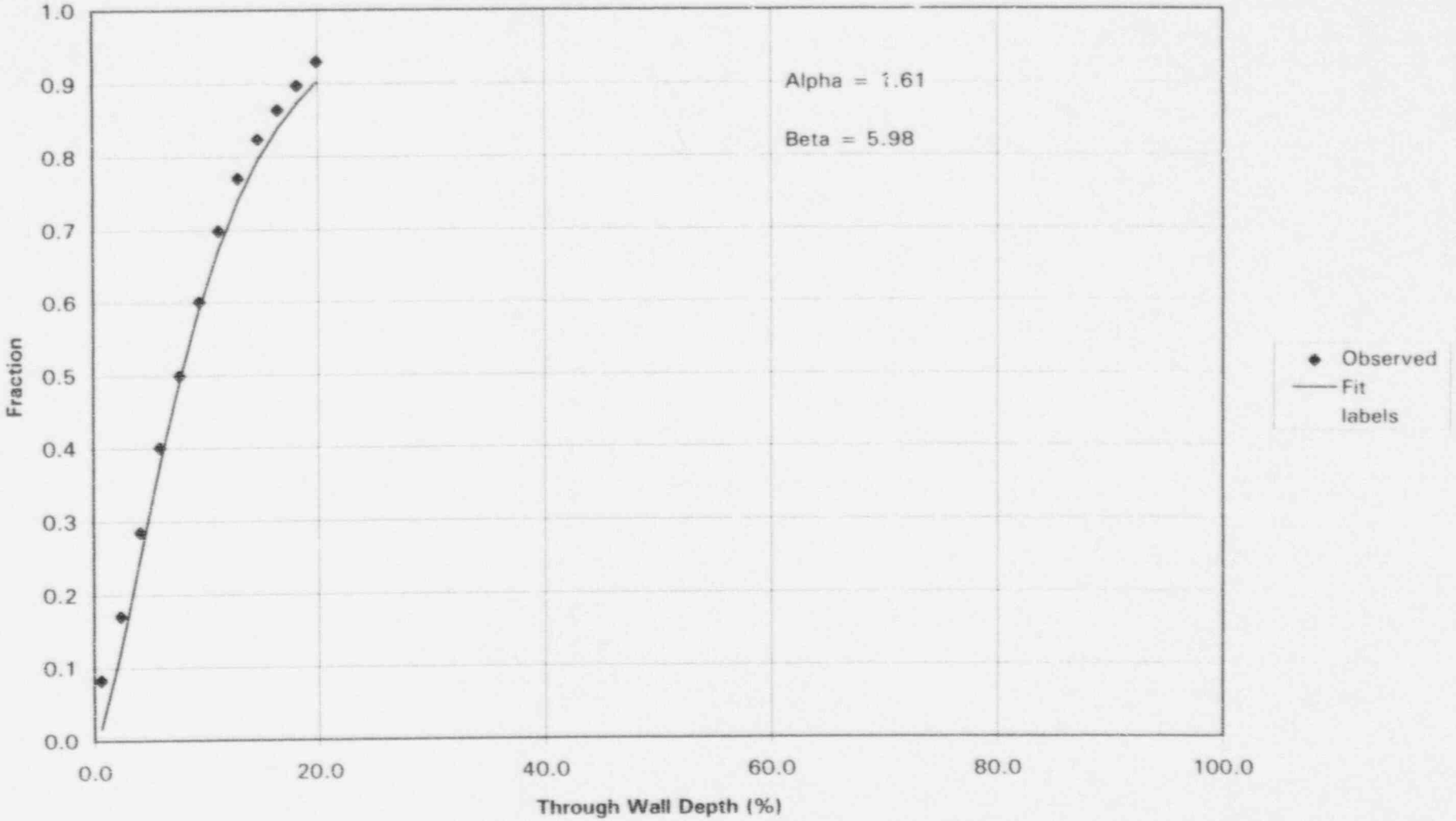

Figure B-13C. Estimated Crack Depth Due to Axial ODSCC at TSPs

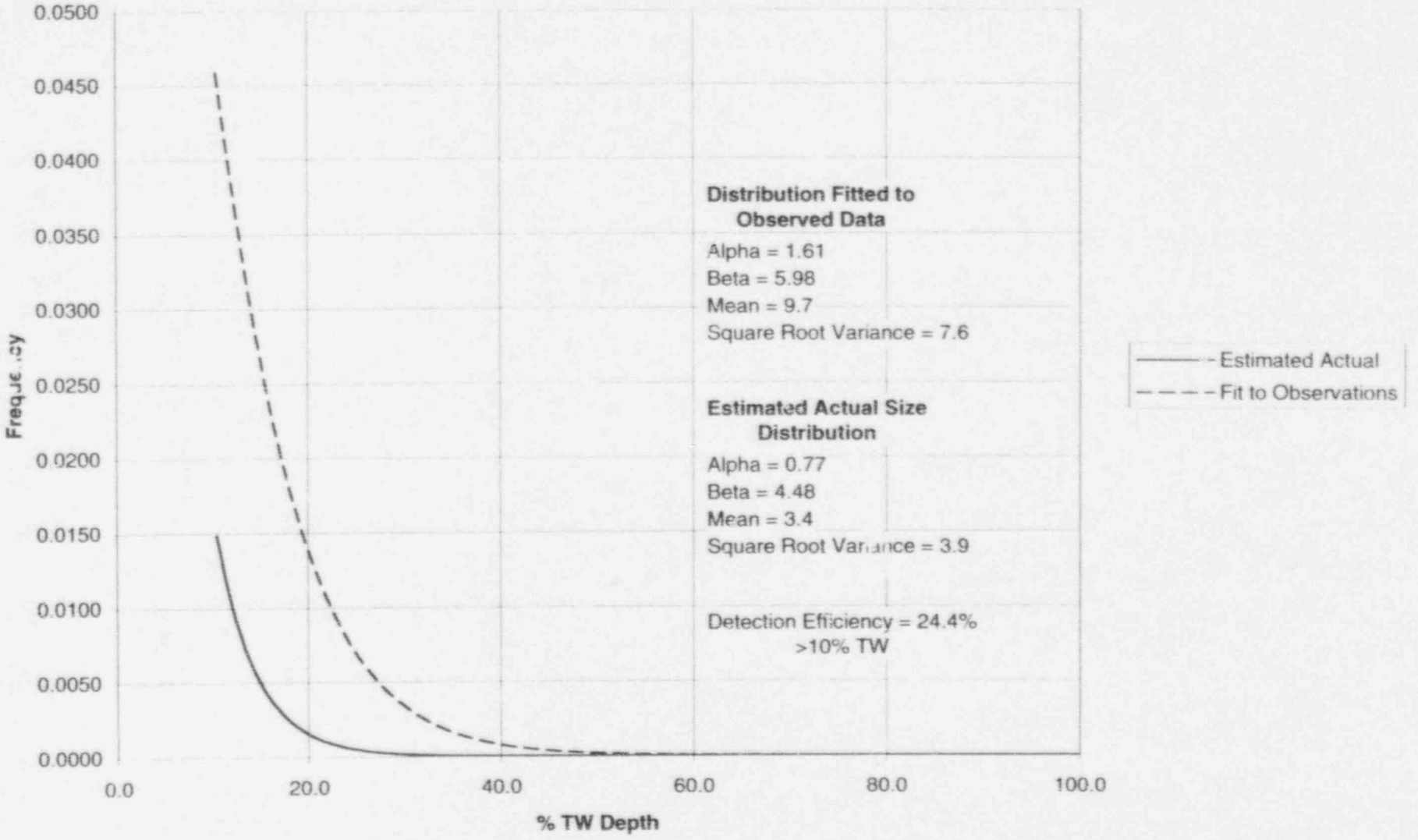

Figure B-13D. Estimated Crack Depth Due to Axial ODSCC at TSPs

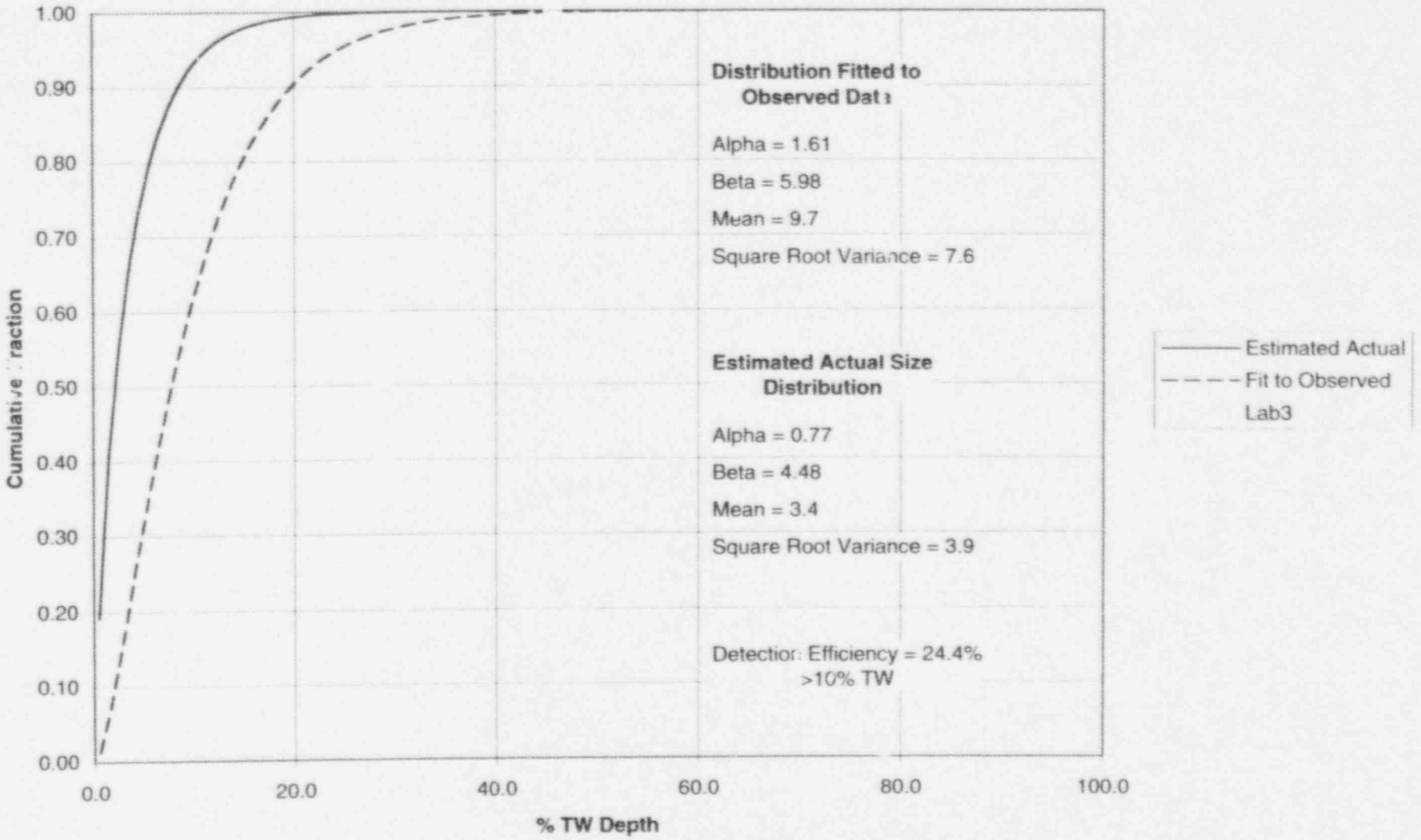

Figure B-13E. Axial TSP Defects - Probabil ty of Detection

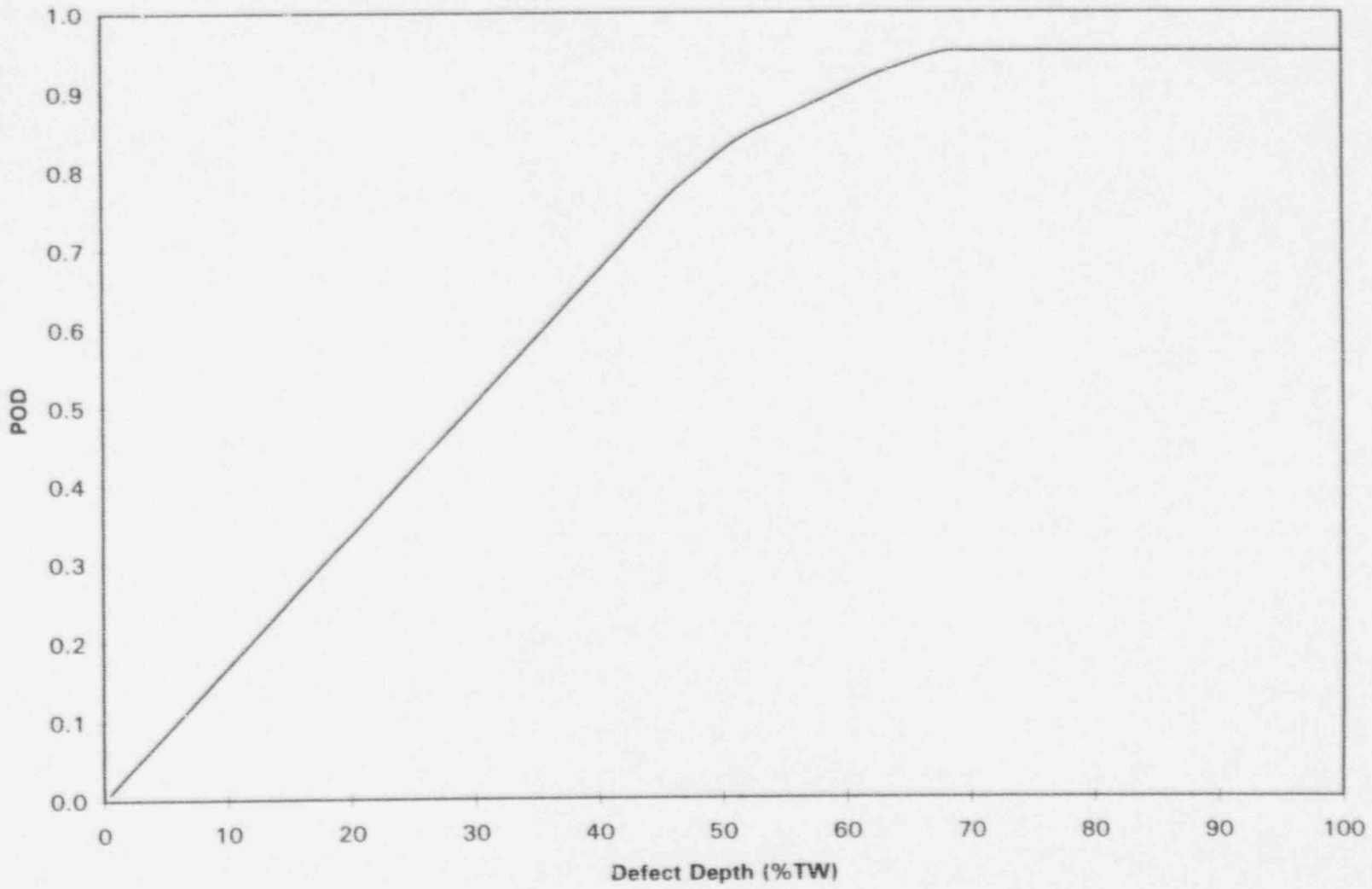

Figure C-16. Binned Flaw Distributions
Axial Crack Depths at TSPs
(Assumed Crack Length of 0.75 inches)

Case:		Moderate	Severe	Light
Detected Flaws:		139.0	1470	32
Detection Efficiency:	0.244			
Total Flaws:		569.7	6024.6	131.15
Alpha:	0.770			
Beta:	4.480			

Depth, % of Wa	F	No. in Bin	No. in Bin	No. in Bin
10	0.00000	0.0	0.0	0.0
11	0.21324	121.5	1284.7	27.97
12	0.38028	95.2	1006.3	21.91
13	0.51136	74.7	789.7	17.19
14	0.61437	58.7	620.6	13.51
15	0.69543	46.2	488.3	10.63
16	0.75928	36.4	384.7	8.37
17	0.80963	28.7	303.3	6.60
18	0.84936	22.6	239.4	5.21
19	0.88074	17.9	189.1	4.12
20	0.90554	14.1	149.4	3.25
21	0.92515	11.2	118.2	2.57
22	0.94067	8.8	93.5	2.04
23	0.95295	7.0	74.0	1.61
24	0.96268	5.5	58.6	1.28
25	0.97039	4.4	46.4	1.01
26	0.97650	3.5	36.8	0.80
27	0.98134	2.8	29.2	0.64
28	0.98518	2.2	23.1	0.50
29	0.98823	1.7	18.4	0.40
30	0.99065	1.4	14.6	0.32
31	0.99257	1.1	11.6	0.25
32	0.99410	0.9	9.2	0.20
33	0.99531	0.7	7.3	0.16
34	0.99627	0.5	5.8	0.13
35	0.99703	0.4	4.6	0.10
36	0.99764	0.3	3.7	0.08
37	0.99812	0.3	2.9	0.06
38	0.99851	0.2	2.3	0.05
39	0.99881	0.2	1.8	0.04
40	0.99905	0.1	1.5	0.03
41	0.99925	0.1	1.2	0.03
42	0.99940	0.1	0.9	0.02
43	0.99952	0.1	0.7	0.02
44	0.99962	0.1	0.6	0.01
45	0.99970	0.0	0.5	0.01
46	0.99976	0.0	0.4	0.01
47	0.99981	0.0	0.3	0.01
48	0.99985	0.0	0.2	0.01
49	0.99988	0.0	0.2	0.00
50	0.99990	0.0	0.1	0.00
51	0.99992	0.0	0.1	0.00
52	0.99994	0.0	0.1	0.00
53	0.99995	0.0	0.1	0.00
54	0.99996	0.0	0.1	0.00
55	0.99997	0.0	0.0	0.00
56	0.99998	0.0	0.0	0.00
57	0.99998	0.0	0.0	0.00
58	0.99998	0.0	0.0	0.00
59	0.99999	0.0	0.0	0.00
60	0.99999	0.0	0.0	0.00
61	0.99999	0.0	0.0	0.00
62	0.99999	0.0	0.0	0.00

Figure C-16. Binned Flaw Distributions
Axial Crack Depths at TSPs
(Assumed Crack Length of 0.75 inches)

Case:		Moderate	Severe	Light
Detected Flaws:		139.0	1470	32
Detection Efficiency:	0.244			
Total Flaws:		569.7	6024.6	131.15
Alpha:	0.770			
Beta:	4.480			

Depth, % of Wall	F	No. in Bin	No. in Bin	No. in Bin
63	0.99999	0.0	0.0	0.00
64	1.00000	0.0	0.0	0.00
65	1.00000	0.0	0.0	0.00
66	1.00000	0.0	0.0	0.00
67	1.00000	0.0	0.0	0.00
68	1.00000	0.0	0.0	0.00
69	1.00000	0.0	0.0	0.00
70	1.00000	0.0	0.0	0.00
71	1.00000	0.0	0.0	0.00
72	1.00000	0.0	0.0	0.00
73	1.00000	0.0	0.0	0.00
74	1.00000	0.0	0.0	0.00
75	1.00000	0.0	0.0	0.00
76	1.00000	0.0	0.0	0.00
77	1.00000	0.0	0.0	0.00
78	1.00000	0.0	0.0	0.00
79	1.00000	0.0	0.0	0.00
80	1.00000	0.0	0.0	0.00
81	1.00000	0.0	0.0	0.00
82	1.00000	0.0	0.0	0.00
83	1.00000	0.0	0.0	0.00
84	1.00000	0.0	0.0	0.00
85	1.00000	0.0	0.0	0.00
86	1.00000	0.0	0.0	0.00
87	1.00000	0.0	0.0	0.00
88	1.00000	0.0	0.0	0.00
89	1.00000	0.0	0.0	0.00
90	1.00000	0.0	0.0	0.00
91	1.00000	0.0	0.0	0.00
92	1.00000	0.0	0.0	0.00
93	1.00000	0.0	0.0	0.00
94	1.00000	0.0	0.0	0.00
95	1.00000	0.0	0.0	0.00
96	1.00000	0.0	0.0	0.00
97	1.00000	0.0	0.0	0.00
98	1.00000	0.0	0.0	0.00
99	1.00000	0.0	0.0	0.00
100	1.00000	0.0	0.0	0.00
	sums	569.7	6024.6	131.1

6. Flaws Due to Loose Parts - Wextex Units

As discussed in Appendix D, the frequency of loose parts events for units that are thoroughly inspected on a frequent basis is about 0.046 per steam generator cycle, and about 5 tubes are involved in each event. For a Wextex unit with three steam generators, this amounts to an average of 3 x .046 x 5 = 0.7 tubes per cycle.

The depth and length distributions suggested for loose parts flaws are shown in Figures D-2 and D-3.

Distributing the numbers of flaws expected at the end of the operating cycle into size bins is not practical since there are two independent size distributions. The user will have to determine the probability of having a defect with both a large length and a large depth using Monte Carlo sampling or equivalent of the two distributions.

Appendix D
Flaws Due to Loose Parts

The objective of this appendix is to quantify the likelihood of flaws due to loose parts (LPs) of various sizes being present in steam generators at the end of an operating cycle. The effects of reduced or less intense inspections on the probability of loose part events (LPEs) is addressed in a preliminary fashion.

Loose parts in steam generators (SGs) have required repair of substantial numbers of tubes, and have resulted in occasional leaks, and two ruptures. The occurrence of LP damage seems to be largely a random occurrence. Somewhat surprisingly, there does not seem to be a noticeable correlation with SG inspection history, since newer plants that have been subjected to less intense inspections (less frequent and/or partial inspections) have not experienced higher rates of leakage or rupture events than the more intensively inspected units. Nevertheless, concern remains that the probability of larger flaws due to loose parts being present could increase as inspection intensity is decreased. This appendix is an initial effort directed at developing a model for assessing this concern. In the longer term, it may be desirable to develop a more detailed mechanistic model that takes into account the likely growth characteristics of LP flaws, and that also models the likelihood of detection as a function of flaw size and inspection practices.

A review of EPRI tube plugging data through 1994[1] indicates the following for recirculating PWR steam generators with alloys 600 or 690 tubes covered by the EPRI data:

Total plant years:	2165
Total SG Years:	6340
Total tubes plugged for LP wear:	972

For this same set of plant experience, two ruptures and 18 leakage events were identified.[2] Since complete data on leakage events was not available, it is assumed that the number of leakage events probably was actually in the neighborhood of 30. Based on the depth and length of flaws required to cause rupture at typical normal operating primary to secondary differential pressures, the flaws involved in the two ruptures are considered to have been equivalent to axial cracks of 2.15 inches or longer with wall penetrations of 90%

---

1 B. L. Dow, Jr., Steam Generator Progress Report, Revision 11, EPRI Nov. 1995.

2 Annual EPRI Steam Generator Progress Reports, AECL reports 4449, 4753, 5013, 5242, 7251, 7689, 8179, & 9107, periodic EdF reports at EPRI meetings, and NRC (Murphy) draft review of rupture experience.

or more. The 30 leakers are assumed to have had 100% of wall penetrations, and variable lengths.

Measured LP flaw depths are available for a set of four units (proprietary data). A gamma distribution was fitted to these data, with the results shown on Figures D-1 and D-2. This gamma distribution was taken as being typical for the industry. It indicates that 3% of the LP flaws will be 100% of wall in depth, which is consistent with the industry leakage history discussed above (i.e., .03 x 972 = 29 leakage events).

The above LP flaw data were approximated using the depth distribution of D-1 and 2 and the length distribution shown on Figure D-3. The two distributions were assumed to be independent, i.e., depth was assumed to be independent of length. The parameters of the gamma distribution for flaw length shown on D-3 were selected by trial and error using Monte Carlo methods to result in an average of two bursts per 1000 flaws. Burst was defined as occurring when the flaw length exceeded 2.15 inches and the flaw depth exceeded 90% of wall in the same trial.

Adjustment of the flaw distributions to account for measurement error and POD was not performed since the distributions were normalized to provide results consistent with industry leakage and burst experience. Thus, the distributions represent actual and not measured sizes without adjustment.

Based on the above, it is recommended that loose part flaw sizes be modeled using independent gamma distributions for depth and length, with the following parameters:

Distribution	Depth, % Wall	Length, in.
Alpha	2.275	1.900
Beta	17.235	.458

In order to estimate the number of flaws present at the end of an operating cycle, it is suggested that the following approach be taken:

- For moderately and severely affected units, the tube plugging, leakage and rupture data cited above are assumed to apply since these units are intensively inspected. For these units, the probability of an LPE is approximated by the following:

  - Each LPE is assumed to involve 5 tubes. Using this assumption, there have been about 972/5 = 194 LPE.

- Since typical operating cycles are about 1.5 years long, the number of steam generator cycles (SGC) ~ 6340/1.5 = 4227.

- The frequency of LPE per SGC = 194/4227 = .046

In summary, for units inspected on a thorough and frequent basis (applicable to most plants with 600MA tubes), it is suggested that the probability of LPEs be modeled as being 0.046 per SGC, and that each LPE be taken as involving 5 tubes. It is suggested that the size and depth distributions of these flaws be modeled as described earlier.

- For SGs that are inspected at less frequent and complete rates the likelihood of a LPE is likely to increase as time progresses, since more chances of entry of LPs occur without them being detected. For example, for a SG that is inspected using a 20% random sample per cycle, the probability of a LPE will be approximately as follows:

Time	Prob. of No LPE	Prob. of LPE
EOC 1	.954	.046
BOC2	.2 + .8(.954) = .963	.0368
EOC2	(.2 + .8(.954)).954 = .919	.0811
BOC3	.2 + .8(.919) = .935	.0649
EOC3	(.935).954 = .892	.1079
BOC4	.2 + .8(.892) = .914	.0863
EOC4	.954(.914) = .872	.1284
BOC5	.2 + .8(.872) = .897	.1027
EOC5	.954(.897) = .856	.1440

It is suggested that the increasing probability of a LPE in a SG subjected to partial inspections be modeled using the above approach, with each LPE involving 5 tubes. It is further suggested that the flaw distributions described earlier be used. This amounts to increasing the number or likelihood of tubes being affected by LP damage, but not changing the flaw size distributions, such that the likelihood of a leak or rupture is controlled by the number of affected tubes and not by the growth in size of individual flaws. It could be argued that the average sizes of LP flaws should also increase, as well as the likelihood of occurrence. However, a qualitative review of

plant experience indicates that, in fact, SGs subjected to partial inspections have not experienced deeper or bigger LP flaws.

Figure D-1. Measured Depths of Loose Part Wear

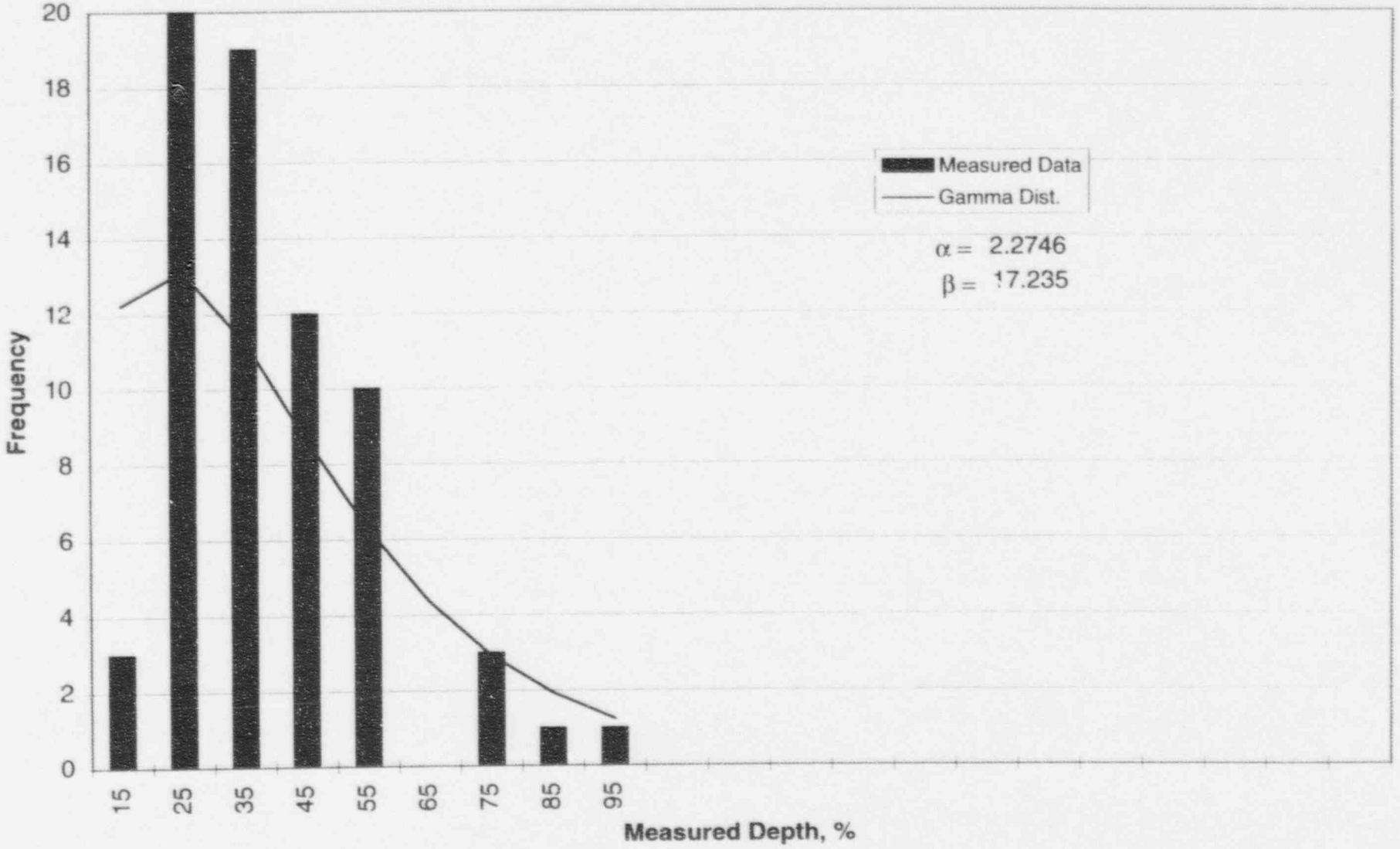

Figure D-2. Cumulative Depth Distribution for Loose Part Flaws

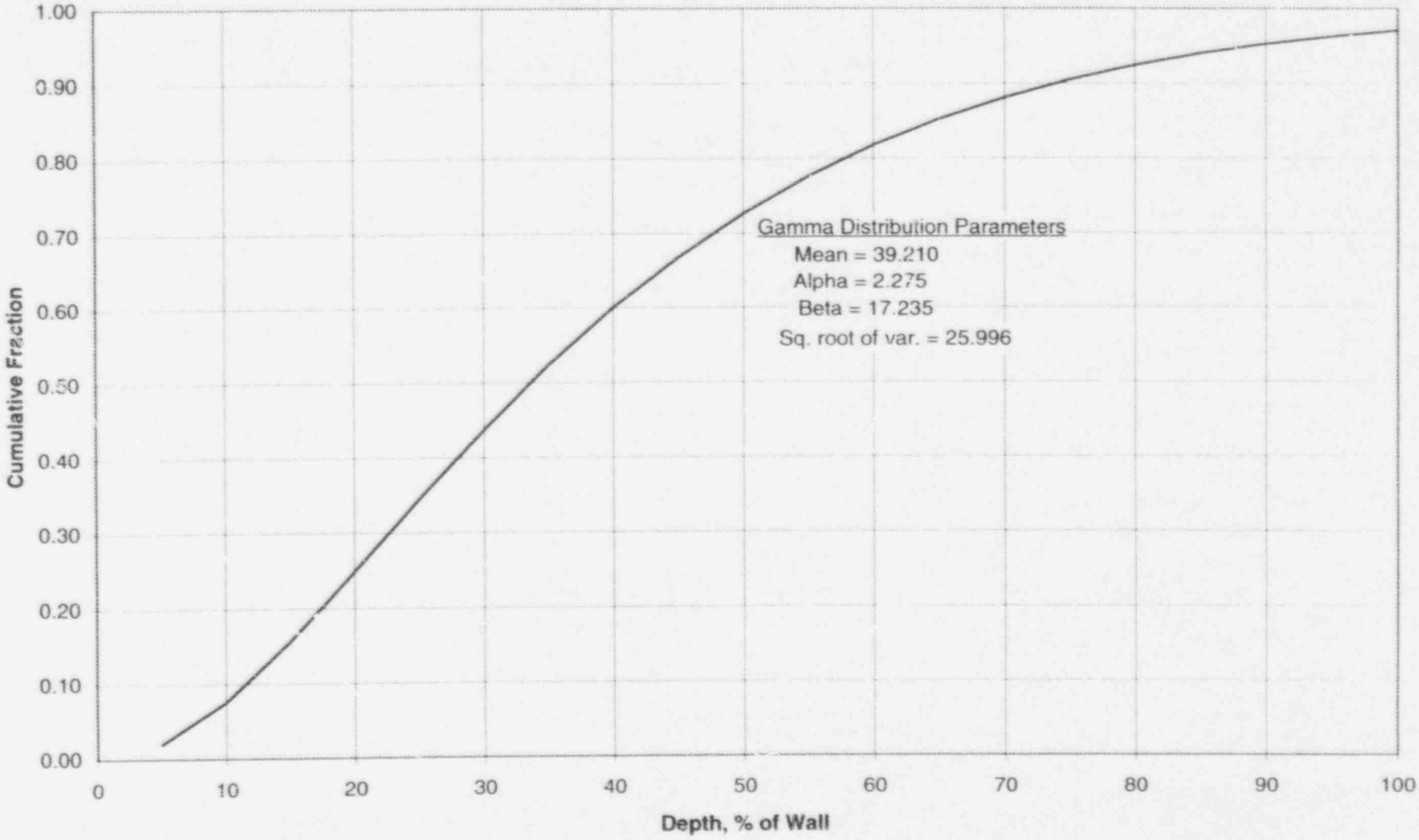

Figure D-3. Cumulative Length Distribution for Loose Part Flaws